ORNL/Sub-4005/1
(IITRI-C6313-14)

PREDICTION OF CAVITY GROWTH BY SOLUTION OF SALT AROUND BOREHOLES

Richard H. Snow
Davy S. Chang

Illinois Institute of Technology
Research Institute
10 West 35th Street
Chicago, Illinois 60616

This report was prepared by the Illinois Institute of Technology Research Institute (IITRI) under subcontract 4005 witn Union Carbide Corporation, Nuclear Division, a United States Atomic Energy Commission (AEC) contractor. The work was further identified as Amendment No. 1, Task Order No. 93, under IITRI's contract E(11-1)-578 with the USAEC. Subcontract 4005 was administered by the Oak Ridge National Laboratory.

Prepared for
OAK RIDGE NATIONAL LABORATORY
operated by
UNION CARBIDE CORPORATION
for the
ENERGY RESEARCH AND DEVELOPMENT ADMINISTRATION

Report No. IITRI C6313-14

PREDICTION OF CAVITY GROWTH BY
SOLUTION OF SALT AROUND BOREHOLES

Union Carbide Corporation
Nuclear Division
P. O. Box M
Oak Ridge, Tennessee 37830

Attention: Dr. W. McClain

Prepared by

Richard H. Snow
Davy S. Chang

IIT Research Institute
10 West 35th Street
Chicago, Illinois 60616

June 30, 1975

FOREWORD

This final report presents the results of an investigation of the growth of cavities by solution of salt around boreholes. It includes the mathematical basis for a computer model of the solution process applicable to this problem, the calibration of the model with data from the Detroit Cavity Experiment, and prediction of cavity size and shape for long times. Additional effects that might be important are discussed, to give an indication of the limitations of the predictions. Some topics for further research are discussed, but the work that was planned is completed and is included in this report.

The authors thank the following personnel of Union Carbide Corporation for helpful discussion and guidance during the project: Dr. William McClain, George Brunton, Dr. Tom Lomenick; and John Schreiber of ERDA. We also thank the Solution Mining Research Institute, Horace Diamond, President, for permission to use the experimental data from the Detroit Cavity Experiment.

The project was conducted under subcontract 4005, task order 93 under contract No. E(11-1)-578 with the U.S. Atomic Energy Commission (now ERDA).

Prepared by

Richard H. Snow
Engineering Advisor
Chemical Engineering Research

Davy S. Chang
Associate Engineer
Chemical Engineering Research

Approved by

Edward G. Fochtman
Manager
Chemical Engineering Research

ABSTRACT

A mathematical model is developed to simulate the process of salt dissolution in a salt formation. The calibration of this model using Detroit Mine data is done systematically by the method of nonlinear regression. The brine concentrations calculated from the regression fit the measured data from Detroit Mine experiment within 10 percent. Because the Detroit data includes periods when the inlet flow is shut off, the agreement with Detroit data indicates that the model adequately represents natural convection effects to predict the cavity growth at very slow feed rates.

The prediction has been done to calculate the cavity growth at feed rate of one gal/hr and one gal/day over a period of 10,000 yr. The result of the prediction shows that the cavity growth is a wide-flaring type and that the significant growth of the cavity only occurs at top layer. The prediction involves a very great extrapolation of time from the Detroit data, but it will be valid if the mechanism of solution does not change. This subject is discussed in the report, and we believe that the prediction is basically correct.

TABLE OF CONTENTS

LIST OF TABLES AND FIGURES

1. INTRODUCTION

ORNL has had an interest in the aspects of cavity growth by dissolution of salt around boreholes. This interest is related to the concern of the possibility of contamination of a radioactive waste repository by the natural circulation of water in nearby abandoned oil and gas holes, which will dissolve a salt formation. Part of the ORNL current program in this area is the development of a mathematical model to simulate the process of salt dissolution within a borehole. The mathematical model is used to predict the size and shape of the cavity over a period of 10,000 years.

This work has been carried out by IIT Research Institute. The general approach of this work is to derive a lumped model incorporating several empirical equations, which characterize the mechanism of salt dissolution and boundary layer flow at the wall. We then calibrated this model using data from the Solution Mining Research Institute (1969) solution mining experiment carried out in the Detroit Mine. This model could then be used for the interests of ORNL.

2. MATHEMATICAL MODELING

In this section we derive a lumped model for the solution process. Figure 1 is a diagram of a cavity that will grow as a result of water entering a borehole. In this investigation, we only consider the case of fresh water originating at the top and being withdrawn to another aquifer at the bottom of the salt cavity.

Withdrawal of brine from the bottom of the cavity causes a downward flow in the bulk of the cavity. As a result, the flow in the bulk of the cavity can be described as a piston-or plug-flow. According to laboratory observations (Snow and Nielsen, 1970), a thin boundary layer, formed by the dissolved salt, creates natural convection on the wall. This boundary layer only flows a short distance down the cavity along the wall and then develops into eddies which consequently mix into the bulk.

Our objective is to calculate the rate of growth and shape of the cavity. To do this, we must also calculate the flow within the bulk of the cavity and the bulk brine concentration profile, since the latter affects the solution rate at each depth. Separate equations govern the salt mass balance and the continuity of the fluid flow, and several empirical equations are needed to represent the rate of salt dissolution.

2.1 Rate of Salt Dissolution

The dissolving rate of salt is obtained from the mass-transfer coefficient and the salt concentration difference

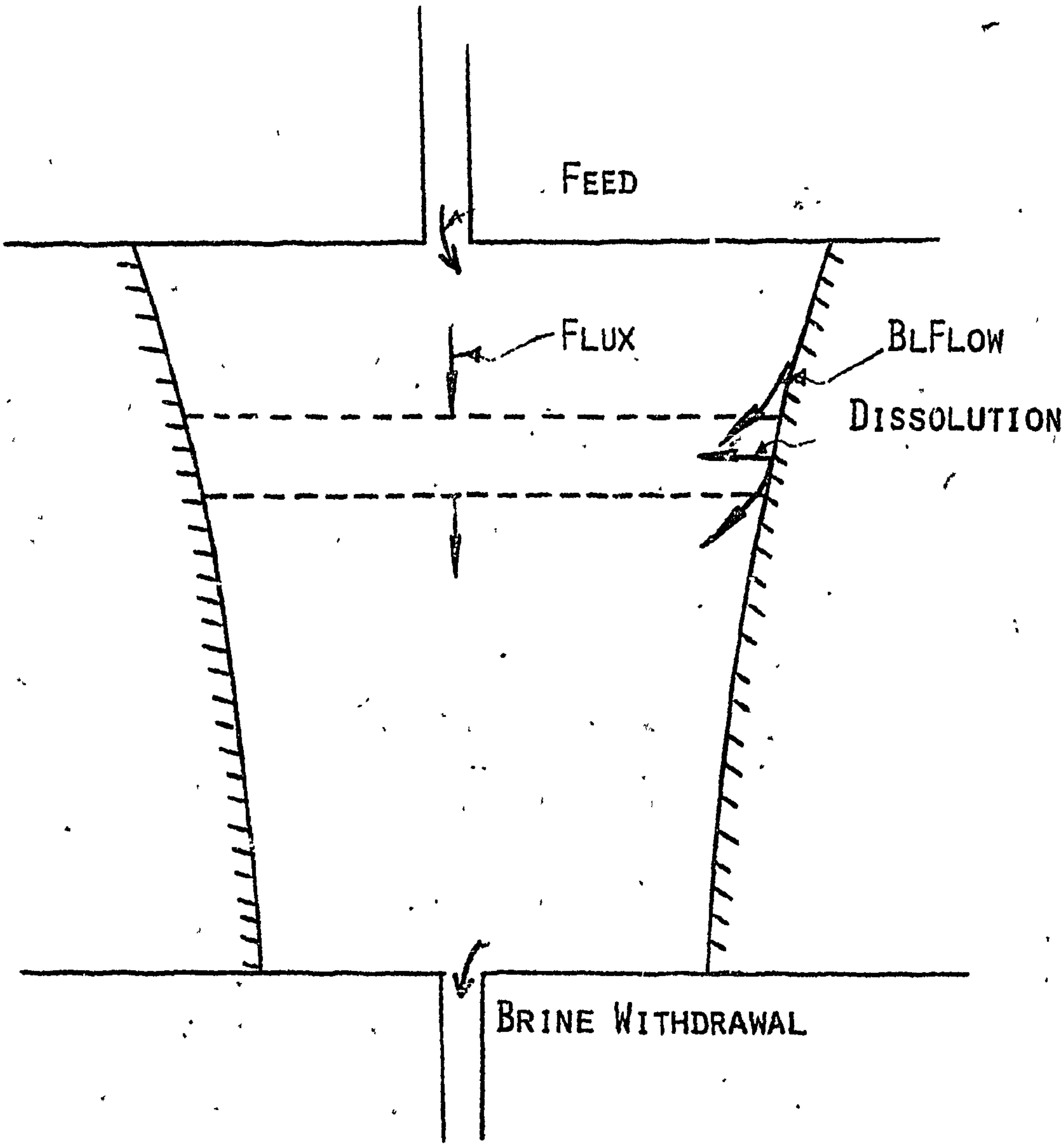

FIGURE 1

DIAGRAM OF SALT CAVITY AROUND A BOREHOLE

$$\text{Solution rate} = K_c(Y^* - Y) \quad (1)$$

where

K_c is mass transfer coefficient,

g salt/(cm^2-mass fraction-sec)

Y is mass fraction of salt in bulk of solution,

g salt/g solution

Y^* is salt solubility at existing temperature,

g salt/g solution

Note that the regression rate of the salt surface is equal to

$$\text{Regression rate} = \frac{\text{Solution rate}}{\rho_s} \quad (2)$$

where ρ_s is salt density, g/cm^3

Saberian (1974) has expressed the rate of solution from laboratory data in terms of a polynomial of solution density, which in turn is a function of $(Y^* - Y)$. The data is plotted on p. 25 of his report. The function is

$$\text{Regression rate} = .7609\rho^4 - 3.872\rho^3 + 7.825\rho^2 - 7.840\rho + 3.880 - 7.534\rho^{-1} \quad (3)$$

This function is concave upward, which suggests that it could be represented by an exponent of $(Y^* - Y)$. A reasonable fit is obtained from the following function:

$$\text{Regression rate} = 2.8\text{x}10^{-3}\ (Y^* - Y)^{1.5}$$

But, from Eq. (2)

$$\text{Solution rate} = \rho_s \cdot \text{regression rate}$$

or

$$K_c(Y^* - Y) = 2.8\text{x}10^{-3}\ \rho_s\ (Y^* - Y)^{1.5}$$

hence,

$$K_c = 2.8\text{x}10^{-3}\ \rho_s\ (Y^* - Y)^{.5}$$

or

$$K_c = K_c'\ (Y^* - Y)^{.5} \qquad (4)$$

2.2 Salt Mass Balance

Consider a salt mass balance in an element of depth (Δx) of the cavity in Figure 1

$$\begin{bmatrix}\text{Accumulation} \\ \text{of salt in the} \\ \text{element}\end{bmatrix} = \begin{bmatrix}\text{Rate of salt} \\ \text{influx}\end{bmatrix} - \begin{bmatrix}\text{Rate of salt} \\ \text{outflux}\end{bmatrix} + \begin{bmatrix}\text{Rate of salt in} \\ \text{by boundary flow}\end{bmatrix} - \begin{bmatrix}\text{Rate of salt out} \\ \text{by boundary flow}\end{bmatrix} + \begin{bmatrix}\text{Rate of salt in} \\ \text{by dissolution}\end{bmatrix}$$

It can be written in mathematical form as:

$$\frac{\partial}{\partial t}\,[\pi r^2 \Delta x \rho Y]_x = (\text{FLUX} \cdot Y)_x - (\text{FLUX} \cdot Y)_{x+\Delta x} + \text{BLFLOW} \cdot \bar{Y}\Big|_x - \text{BLFLOW} \cdot \bar{Y}\Big|_{x+\Delta x} + 2\pi r \Delta x K_c (Y^*-Y)\Big|_x$$

Divide the above equation by Δx and take the limit as $\Delta x \to 0$

$$\frac{\partial}{\partial t}(\pi r^2 \Delta x \rho Y) = -\frac{\partial}{\partial x}(\text{FLUX} \cdot Y) - \frac{\partial}{\partial x}(\text{BLFLOW} \cdot \bar{Y}) + 2\pi r K_c (Y^* - Y) \qquad (5)$$

where

FLUX is mass flow rate in bulk of cavity, g solution/sec

BLFLOW is boundary layer mass flow rate, g solution/sec

$\bar{Y}$ is mean concentration in the boundary layer, g salt/g solution

2.3 Boundary Layer Flow (BLFLOW)

The amount of salt carried in the BLFLOW is determined by the salt solution rate and by the distance h through which the boundary layer carries the salt. Therefore, the amount of freshly dissolved salt being carried at any point in the boundary layer is the amount of salt dissolved in the layer within the length h. By the law of conservation of mass this can be equated to

$$(\bar{Y} - Y)\ \text{BLFLOW} = h\ (\text{solution rate})$$

or

$$(\bar{Y} - Y)\ \text{BLFLOW} = 2\pi r h K_c (Y^* - Y) \qquad (6)$$

We expect that h will increase with decreasing $(Y^* - Y)$ since the boundary layer flow is observed to become more nearly laminar with less frequent eddies as the concentration driving force becomes smaller. The following function has this required behavior

$$h = \frac{1}{B'(Y^* - Y)^{b'}} \qquad (7)$$

Furthermore, BLFLOW should increase with increasing solution rate, because the added salt increases the mass of the boundary layer and increases the density force which causes convection. The following function has this required behavior

$$BLFLOW = C'[2\pi r K_c' (Y^{*}-Y)^{c}] \qquad (8)$$

2.4 Equation of Continuity for the Solution

As we mentioned, the flow is assumed to be piston-flow in the bulk of the cavity. Therefore, the equation of continuity for the solution can be written with terms similar to those above for the salt.

$$\begin{bmatrix}\text{Accumulation of mass}\\ \text{in the cell as it}\\ \text{changes in solution}\\ \text{density and grows in}\\ \text{volume}\end{bmatrix} = \begin{bmatrix}\text{Rate of mass}\\ \text{influx}\end{bmatrix} - \begin{bmatrix}\text{Rate of mass}\\ \text{outflux}\end{bmatrix} + \begin{bmatrix}\text{Rate of mass in}\\ \text{by boundary}\\ \text{flow}\end{bmatrix} - \begin{bmatrix}\text{Rate of mass}\\ \text{out by bound-}\\ \text{ary flow}\end{bmatrix} + \begin{bmatrix}\text{Rate of mass in}\\ \text{by dissolution}\\ \text{of salt}\end{bmatrix} .$$

Its mathematical form† is

$$\frac{\partial}{\partial t}(\pi r^2 \Delta x \rho)_{x} = \text{FLUX}\Big|_{x} - \text{FLUX}\Big|_{x+\Delta x} + \text{BLFLOW}\Big|_{x} - \text{BLFLOW}\Big|_{x+\Delta x}$$

$$+ 2\pi r K_c (Y^* - Y)\Delta x \qquad (9)$$

Divide the above equation by Δx and take the limit as $\Delta x \to 0$,

$$\frac{\partial}{\partial t}(\pi r^2 \rho) = -\frac{\partial(\text{FLUX})}{\partial x} - \frac{\partial(\text{BLFLOW})}{\partial x} + 2\pi r K_c (Y^* - Y) \qquad (9)'$$

2.5 Salt Regression

The rate of change of the cavity diameter can be expressed from the rate of salt regression, i.e.:

$$\frac{\partial r}{\partial t} = (Y^* - Y)\frac{K_c}{\rho_s} \qquad (10)$$

---

†Although this equation is written in terms of mass, it is derived from the concept that the amount of solution in the element depends on the volume of the element. It is critical that the terms in this equation be properly expressed if the model is to correctly represent the flow behavior of brine in the cavity. The basic equation in terms of volume is

$$\text{Change in volume of element} = \frac{1}{\rho}\begin{Bmatrix}\text{accumulation}\\ \text{of mass}\end{Bmatrix} = \frac{1}{\rho}\begin{Bmatrix}\text{mass in}\\ -\text{mass out}\end{Bmatrix}$$

The second of these two equalities results in the equation given in the text above Eq. 9.

The left term in Equation 9 gives the model its realistic flow behavior. It takes into account the experimental fact that there is a volume decrease when one gram of salt is dissolved in a given quantity of water. The volume formerly occupied by the salt can now be occupied by brine; hence the increase in radius r. The decrease in volume of water plus dissolved salt is reflected in an increase in density of solution ρ. As a result of this term the model correctly predicts an influx of previously-produced brine into the bottom of the cavity when the fresh feed is shut off at the top.

We also make the assumption that the brine density is approximately linear with its concentration, i.e.:

$$\rho = \rho_{water} + \alpha Y$$

then

$$\frac{\partial \rho}{\partial t} = \alpha \frac{\partial Y}{\partial t} \qquad (11)$$

where α is the solubility of salt in the water at given temperature.

3. NUMERICAL CALCULATION

In Equations 4 to 11 there are eight unknowns, namely Y, $\bar{Y}$, ρ, r, FLUX, BLFLOW, h, and K_c. There are also five parameters, namely B', b, c', c and K_c'. If the values of these five parameters were known, the eight equations with eight unknowns could be solved.

These five parameters were determined by the method of constant estimation. This method uses a regression technique to match the calculated brine concentrations best fitting the experimental data from the Detroit Mine experiment. In the next section we will explain the regression technique.

Substituting Eq 9 and Eq 6 into Eq 5 and reducing gives

$$\pi r^2 \rho \frac{\partial Y}{\partial t} = - \left[FLUX + BLFLOW\right] \frac{\partial Y}{\partial x} + 2\pi r K_c (Y^* - Y)(1 - Y) - \frac{\partial}{\partial x}\left[2\pi r h K_c (Y^* - Y)\right] \quad (12)$$

Substituting Eq 10 and 11, Eq 9 can be reduced to

$$\pi r^2 \rho \frac{\partial Y}{\partial t} = -\frac{\partial}{\partial x}\left[FLUX + BLFLOW\right] + 2\pi r K_c (Y^* - Y)(1 - \frac{\rho}{\rho_s}) \quad (13)$$

Analytical solution is impossible to solve Eq 12 and 13 simultaneously because they are coupled to one another. For this reason, the finite difference method is employed to solve them.

3.1 Finite Difference Solution

The cavity in Figure 1 is divided into N equal elements of depth, Δx. The elements are numbered from 1 to N. Using the backward finite difference method, for any element n at time t, Eq 12 and 13 become

$$\Delta x \pi r^2 \rho \, DYDT_{t,n} = \left[FLUX + BLFLOW\right]_{t,n} \left[Y(n-1) - Y(n) \right]_t$$

$$+ [2\pi r K_c (Y^* - Y)(1-Y)]_{t,n} + [2\pi r h K_c (Y^* - Y)]_{t,n-1}$$

$$- [2\pi r h K_c (Y^* - Y)]_{t,n} \qquad (14)$$

$$\Delta x \pi r^2 \alpha \, DYDT_{t,n} = [FLUX + BLFLOW]_{t,n-1} - [FLUX + BLFLOW]_{t,n}$$

$$+ [2\pi r K_c (Y^* - Y)(1 - \frac{\rho}{\rho_s})]_{t,n} \qquad (15)$$

Eq 14 and 15 together with 7 and 8 are solved iteratively, given the initial conditions and the values of five parameters. It usually takes less than 3 iterations to converge the calculations. These calculations determine the brine concentrations in each element at time t. Then the brine concentrations in each element for the next increment of time are obtained by

$$Y_{t+\Delta t,n} = Y_{t,n} + DYDT_{t,n} \cdot DT \quad \text{for } n=1, 2, \ldots, N$$

and the cavity growth is

$$r_{t+\Delta t,n} = r_{t,n} + (\text{Regression Rate})_n \cdot DT$$

A computer program based on this numerical calculation scheme has been constructed and been found to work satisfactorily. This main program is called SALT. It has been found that this finite difference scheme maintains the stability of the computation when

$$\frac{|u|\Delta t}{\Delta x} < 1 \qquad \text{or} \qquad \Delta t < \Delta x/u_{max} \tag{16}$$

For the practical application, especially for very slow rate of bulk flow, it is found that the optimum Δt is not greater than $1/2\ (\Delta x/u_{max})$.

3.2 Parameter Estimation using Nonlinear Regression Technique

As mentioned previously, there are five parameters in the governing equations. Those parameters empirically represent the characteristics of the mechanism of salt dissolution and boundary layer flow along the wall. Theoretically, this mechanism can be studied in the laboratory in order to determine dissolution rate, mass transfer coefficient, and boundary layer flow. Then one could consider a mixing factor for the purpose of scaling up. However, this approach has several shortcomings: 1) Laboratory study of salt dissolution may not be truly representative of cavity salt dissolution, because it is found that the rate of salt dissolution is a function of bulk velocity, of roughness of salt surface, and even of salt surface inclination; 2) Dynamic similarities between model and cavity are difficult to achieve for the purpose of scaling up a mixing factor; 3) Most important of all, global effects of salt dissolution and mixing may not be additive due to the fact that one affects the other.

Instead of relying on laboratory-scale data, we made use of pilot-scale measurements conducted by the Solution Mining Research Institute. These measurements, referred to as the Detroit Cavity Experiment, were made in an experimentally-developed cavity below the International Salt Company mine in Detroit in 1969. These experiments included measurements of the growth rate of the cavity (by direct probing) over a period of two weeks while measuring the inlet and outlet flow rates and concentrations. In addition, the concentrations in the bulk cavity brine were measured at frequent intervals. An upper limit to bulk flow velocities was measured, and the movement and locations of boundary layer flow eddies was determined by a hot-wire anemometer.

In this program, we fit the experimental data to the computer model, including both the cavity growth rate and the bulk solution concentrations. The latter are a more sensitive measure of the correctness of the boundary layer flow part of the model. What we do is to use a nonlinear regression subprogram (called REGRESSION) incorporated into the main program (called SALT). Then we could systematically estimate parameters such that the calculated brine concentrations best fit the experimental data. At first we assign arbitrary values for five parameters and then use SALT to calculate the brine concentration for each depth of the cavity. The next step is to input calculated brine concentrations along with measured brine concentrations into REGRESSION. Then REGRESSION does the analysis of sensitivity to choose a searching direction for the increment of each parameter. These searching gradients are then stored in a Jacobi matrix, and this matrix is then used to determine increments of all parameters every time new calculated brine concentrations are given to REGRESSION. Numerical calculation is used to update the searching gradient at the same time. The update parameters are then input into SALT to calculate new brine concentrations. This scheme of regression will systematically estimate parameters such that the calculated brine concentrations best fit the measured data.

4. COMPARISON OF CALCULATIONS WITH DETROIT CAVITY DATA

The results of the best regression are shown in Tables 1 and 2 (p.36) ·troit experimental data. Listed in the table at each depth . 0 cm are the cavity radius, the regression rate (rate of dissolving) of the cavity salt wall, the bulk brine concentration Y as computed and as measured during the Detroit Cavity Experiment, the downward mass flow rate in the bulk of the cavity, and the downward velocity corresponding to this flow. Phase I corresponds to the first week of the experiment, when a high feed rate was used. But most of the data we used for the purpose of the regression were during periods of time during Phase I when feed flow was cut off. The agreement of the calculated brine concentrations with experimental data is within 15% as shown in Table 1 and Figure 2.

For example, at 20.5 hr the flow was cut off. Because the dissolut' n of salt on the wall was still continuing, brine concen ·cion within the cavity increased rapidly. It is noted that bulk flow was reversed at this time and then gradually reduced as the brine concentration continued to build up in the cavity. One reason for these effects is because dissolution of salt creates downward flow along the wall due to the natural convection, even with the feed rate cut off. The other reason is because brine solution occupies less volume than its pure components. Therefore, when the feed is cut off, brine solution enters the cavity from the bottom.

Listed in Table 2 are the regression results for Phase II, the second week of the experiment when lower feed rates were used. The agreement is within 10% (see Figure 3). Figure 4 also compares the computed cavity radii with experimental radii. The error is less than 3%.

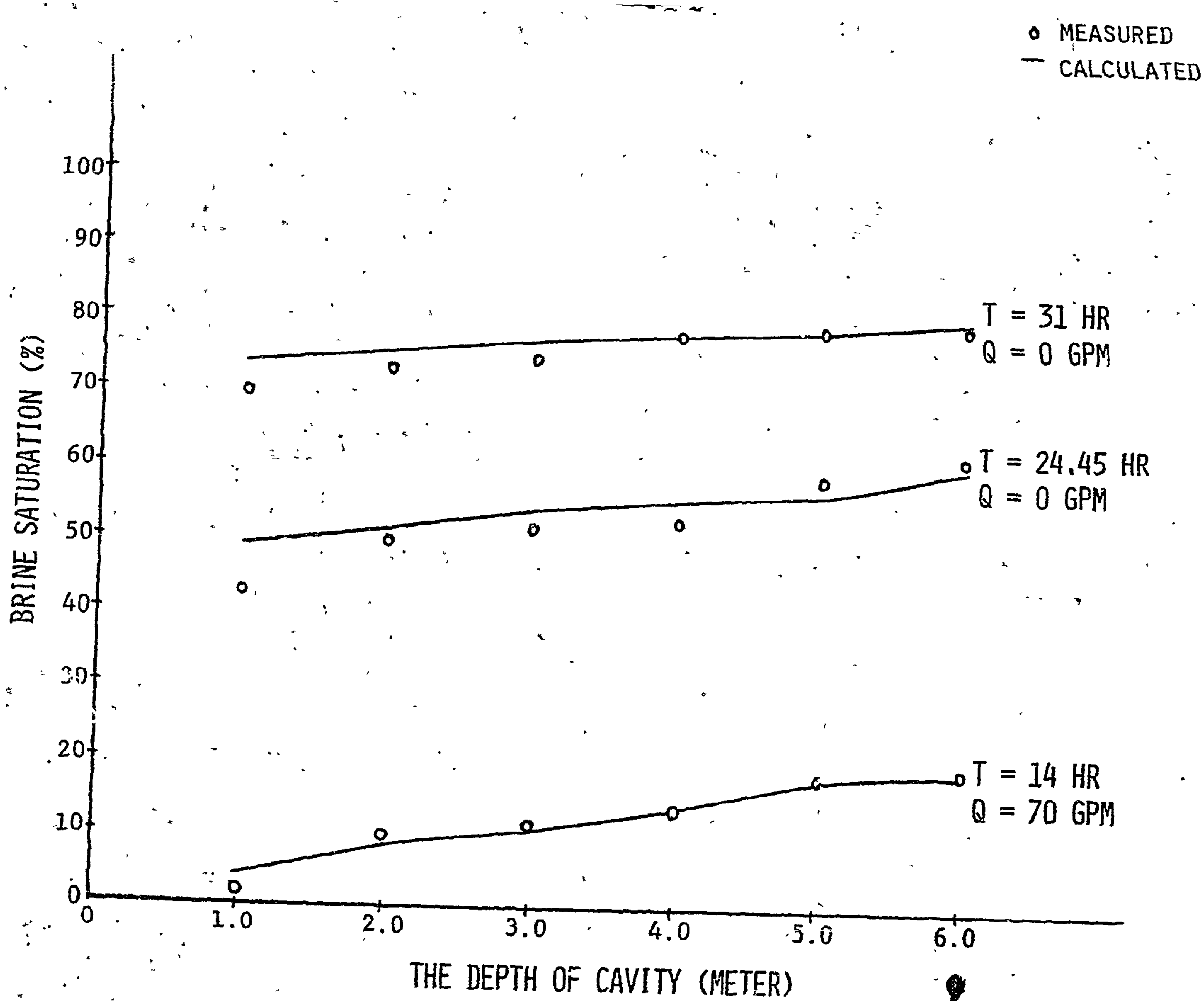

FIGURE 2

REGRESSION RESULT OF PHASE I DATA

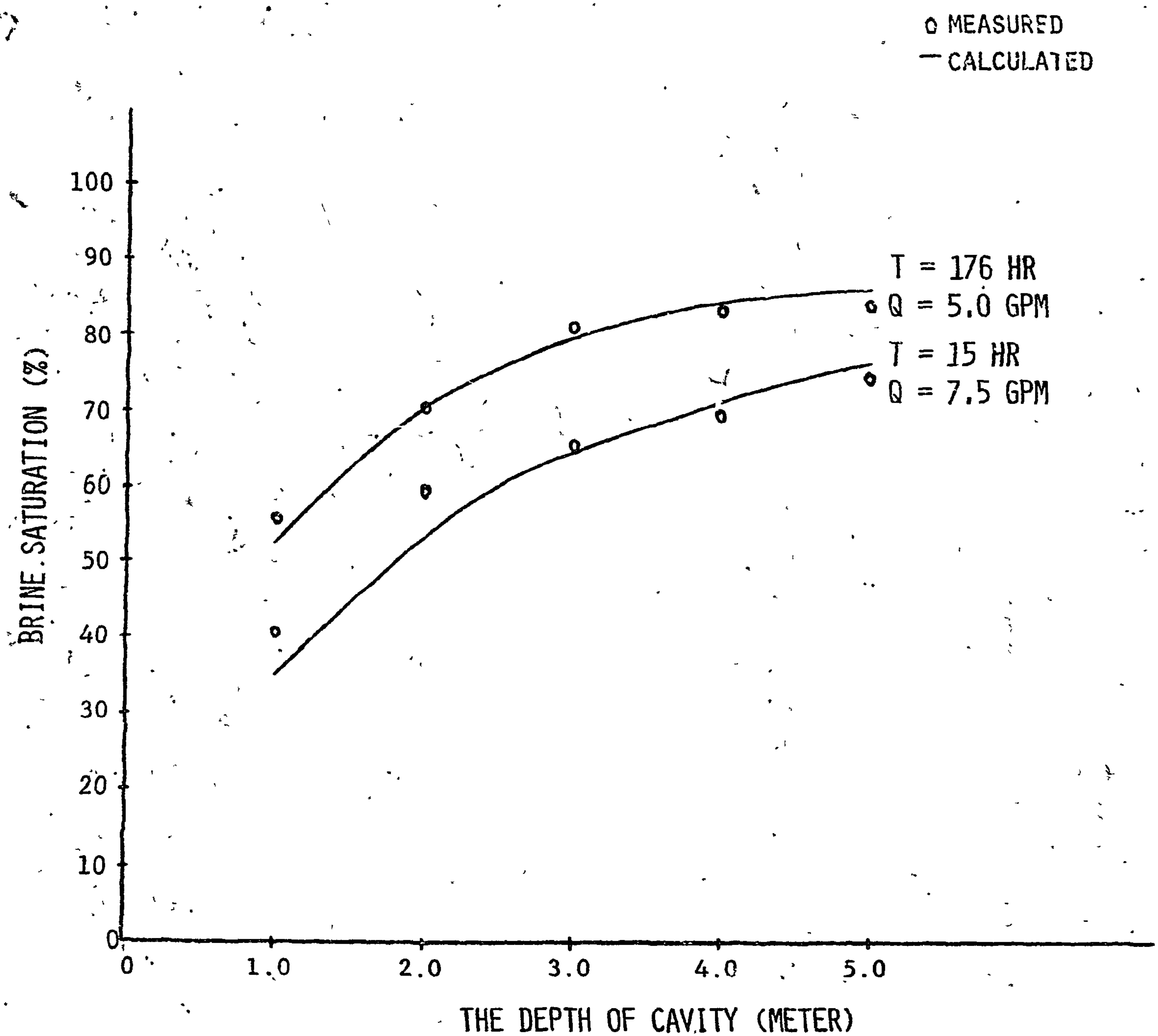

FIGURE 3

REGRESSION RESULT OF PHASE II DATA

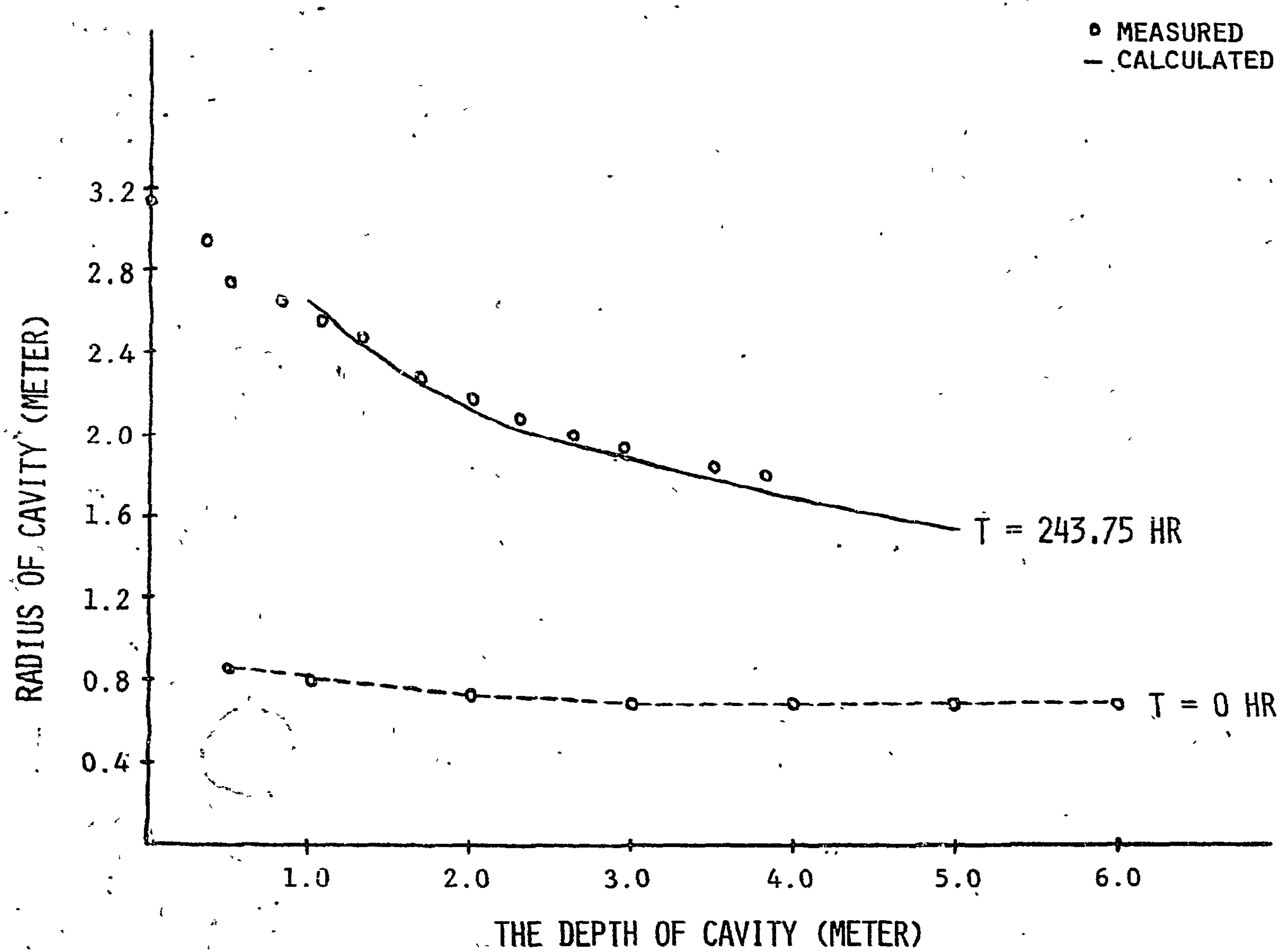

FIGURE 4

FINAL OUTLINE OF THE CAVITY

The results of regression indicate that the mathematical model is sophisticated enough to predict the cavity growth at very slow feed rates, since it agrees with data when the feed is shut off. We will use for subsequent calculations the regression result of Detroit Phase I experimental data. The reason is that Detroit Phase I data were obtained mostly during the time when feed flow was cut off. When feed flow is cut off the natural convection is the dominating mechanism of salt dissolution. If we want to predict the cavity growth at low feed rate this mechanism will be the most important factor of salt dissolution, too.

5. PREDICTION OF CAVITY GROWTH

The mathematical model has been used to predict cavity growth at feed rate of one gal/hr and at one gal/day over a period of 5.7 years.

This prediction started with the injection of the feed flow at 72 gal/min into the cavity with the same initial conditions as Detroit Phase I cavity. This will simulate the case where the borehole is initially open to high flow, and gradually becomes plugged. The feed rate was kept constant for 500 hr and then decreased to 10 gal/min for another 500 hr. At 1000 hr the feed rate was reduced to one gal/min for 1000 hr more. At 2000 hr the feed rate was slowed down to one gal/hr and kept at that feed rate till the calculation ended at the time of 5.7 year.

The result of the prediction is shown in Table 3. The cavity depth is given in increments of 50 cm down to the cavity height of 600 cm. Note that after the bottom portion of the cavity approaches saturation, the significant growth of the cavity occurs at top 50 cm only, and the rate of dissolution is substantial only in this first layer. Another point worth noting is that after the bulk flow reaches a steady rate, the effluent mass flow rate is about 20% higher than the influent feed rate. This is because each cm^3 of salt is replaced by a cm^3 of brine having lower density than salt.

Another computer calculation was done decreasing the feed rate to one gal/day after 2000 hr. The result is shown in Table 4. Generally, the shape of cavity is similar to that in Table 3, except that more time is required to reach the same size.

Although this calculation was only carried out to 5.7 yrs., it can be done for 10,000 yrs. without any difficulty, except that rather long computer runs are required. We did carry out one calculation for 10,000 yrs. at a feed rate of 1 gal/hr. The cost of the computation on a Univac 1108 was $100. The results given in this report are not complete because not all the desired information was printed in the output. We did not repeat the run because we found a more general way of calculating the long-term cavity growth. This more general calculation method is based on the computer print-out showing that the salt dissolution rate becomes steady after some period of time. For example, in Table 3 the dissolution rate becomes steady after 3424 yr. when the feed rate was one gal/hr. In Table 4 it is steady after 5.7 yr. when the feed rate was one gal/day. At these long times the dissolution rate is equal to the amount of salt that can be dissolved by the feed, and so it is proportional to the feed rate. It was also noted that the dissolving took place in the top cell of the cavity only.

For these reasons, we have found a method of calculating cavity growth for long time by hand, after the computer model has shown that the cavity growth reaches a steady rate. The simple equation for this purpose is:

$$\text{Rate of cavity growth} = \frac{\text{Rate of salt dissolution}}{\rho_s}$$

or

$$\begin{array}{c}\text{Increase in volume of}\\ \text{top element of cavity}\end{array} = \begin{array}{l}\text{Salt that can be dis-}\\ \text{solved by amount of}\\ \text{water fed}\end{array}$$

If we write it in arithmetic form, it will be:

$$\pi\Delta(r^2)\ \Delta x\ \rho_s = Q\ \Delta t\ (1.68\times10^3\text{g salt/gal}) \qquad (17)$$

where

Δt is increment of time, hr

Δr is increase of radius in the top cell of the cavity during Δt, m

Q is volumetric feed rate, gal/hr

Δx is top element of cavity depth, cm

This is based on the computer result that each gallon of feed dissolves 1.68 Kg salt. If the initial radius is small compared to the final radius, then

$$\Delta r(m) = 2.22 \times 10^{-2} \sqrt{Q\Delta t} \qquad (17')$$

This equation is expressed graphically in Figure 5.

In the following, we will illustrate this calculation for the cases in Tables 3 and 4.

Case I: Prediction of the cavity size at time T_2 = 11,415 years, if the feed rate

Q = 1 gal/hr

From Table 3, when T_2 = 11,415 yr the radius of the top cell of the cavity = 222.78 m

If we use Eq 17 or Figure 5 to calculate the top cell radius, neglecting the growth of the remaining cells of the cavity, the result is 222.88 m. Thus the error of Eq 17 is slight if $\Delta r_1 > \Delta r_2$.

Case II: Prediction of the cavity size at time T_2 = 11,415 yr, if the feed rate

Q = 1 gal/day

The computer calculation given in Table 4 extended to 5.7 yr. At this time the radius of the top element of the cavity was 11.95 m.

We can use Eq 17 to compute the top element radius at 11,415 yr (10^8hr). The result is 47 m.

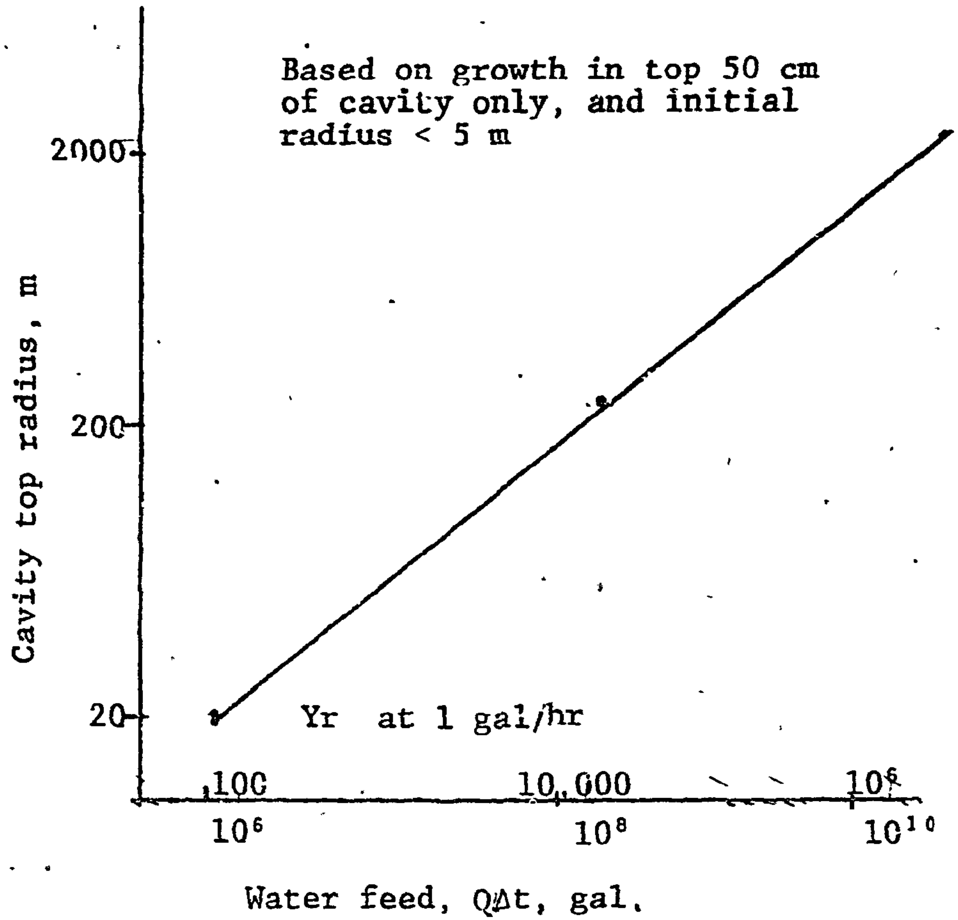

Figure 5. Cavity Growth Prediction

6. DISCUSSION OF PRACTICAL APPLICATIONS OF THE MODEL

It must be recognized that we have extrapolated the model to calculate the shape of salt cavities after long periods such as 10,000 years. The model predicts the growth of a gently flaring cavity over a period of a few weeks with a flow rate of a few gal/min, and the model parameters have been calibrated for these conditions. At very long periods of time the model predicts that essentially all of the cavity growth will occur in the top element of the cavity. The depth of this dissolving element is arbitrary; in our calculations, we have used 50 cm. In additional computer calculations, we explored the effect of element depth, and found that 10 cm or 25 cm elements gave practically the same cavity shape over periods of a week or two. However, over long periods of time, the assumed depth of the top element will have a direct effect on the calculated top element radius. We can discuss the factors that will affect the dissolving depth of the top element, but we do not have reliable data to predict it. To this extent, the results are an estimate.

Table 3 does show that the growth of the second element is slight compared to the growth of the top element. At 11,400 yr, the top element radius is 222 m, while the second element radius is only 11 m.

The actual depth of the top element, in which most of the dissolving takes place, will depend on several effects. The first of these is the dissolving rate. When the cavity is very large, the perimeter of the top element is so great that the amount of salt that can be contained in 1 gal/hr of water fed can be dissolved in a small depth. This depth might be as small as a few cm, if it were not for other effects that can occur.

A second effect is that of mixing of the influent water with the brine in the cavity. At feed rates of 10 gal/min the influent water can have a jet effect that can cause mixing to a depth of 50 cm or more, as was observed in the Detroit cavity experiment. However, at 1 gal/hr, the jet mixing effect should be small, and we have set it equal to zero in the model.

Another effect is that due to the slope of the cavity wall, which is known to decrease the rate of mass transfer (Saberian, 1974) approximately according to the cosine of the declination from vertical. The slope of the cavity in the Detroit experiment was sufficiently close to vertical so that it was not necessary to apply this correction. When extrapolating to a very wide-flaring cavity, the slope should be important. However, other effects may be of equal or greater importance.

Another effect that may change the cavity growth is the occurrance of rock falls from the cavity roof. This is certain to occur as the span widens over long periods of time. However, we believe that this can be neglected as a first approximation. The reason is that, although the rocks will fall into the cavity, it will remain macroscopically porous, and the normal cavity flows can continue with very little effect, especially in the top layer where fresh water first meets the salt face. Some unpublished sonar measurements in large salt-producing cavities (400 ft.diam) indicated that solution was still taking place in spite of massive rock falls reaching nearly to the roof of the cavity.

Another effect is the declination of the bedding plane of the salt due to tilt at some period after the salt was deposited. Even a few degrees tilt can result in one side of the cavity top element being exposed to fresh water while on the other side the top of the salt lies below the fresh water layer, in saturated brine. In this case, dissolution will occur primarily on the uptilt side of the cavity, and the growth will be unsymmetrical. There have been attempts in the literature to develop an assymetrical model of cavity growth, but it seems sufficient to estimate that if one side of the top element is below the dissolving layer, then the salt dissolution will be concentrated at the other side. From the geometry alone, one can estimate that the growth on the dissolving side will be 2 or 3 times the growth that would occur in a circular cavity.

Nolen, et al (1974) reported a 3-dimensional numerical simulation of the solution mining process. Their formulation involved a number of approximations to allow them to reduce the problem to one that could be handled by finite-difference computer simulation. In particular, the flow field was represented by a turbulent eddy diffusivity, and the solution rate was represented by a standard mass transfer coefficient. They used their program to fit the shape of two salt cavities measured by sonar, and thus evaluate the empirical parameters in their model. They mentioned that the model could be used to predict assymetric cavity shapes if it is assumed that the mass transfer coefficient arbitrarily varies with direction (is anisotropic). They postulated that anisotropy might be due to dip in the bed plane, but gave no way to estimate this effect.

Any boundary layer model of the solution process implies that the rate of solution varies slowly down the depth of the cavity wall. Actually, the boundary layer forms over a depth of 2 or 3 cm of the salt face. The salt at the top of the face is exposed to solution with a very sharp concentration gradient normal to the face, and the solution rate is relatively high there. Laboratory experiments (Snow, 1969) indicated solution rates about twice as high at the top compared to further down the salt face. In the Detroit cavity experiment, it was observed that a top layer of salt 2 or 3 cm deep dissolved back about 1 ft further than the rest of the salt face, probably for this same reason. If this effect were to continue at the same rate for 10,000 yr, then the progress of this narrow layer could extend very far. However, this does not seem likely, because the detritus from the dissolved salt would tend to block the flow of fresh solution into this layer, even more than into a layer assumed to be 50 cm deep. Because of this detritus, we think it very unlikely that such a narrow top layer could progress more than a few tens of ft beyond the main salt face.

Another effect is that due to molecular diffusion causing mixing of salt into the top element of the cavity from the nearly-saturated brine below the top element. This effect is not significant in a cavity of the size encountered in the Detroit experiment, but it might become important in a cavity growing over a period of 10,000 years.

This can be calculated from

$$D\frac{\Delta(\rho Y)}{\Delta x}\pi r^2 = q \qquad (18)$$

where

Δx is the thickness of the top element which contains unsaturated brine

D is diffusion coefficient of salt, 1.15×10^{-5} cm^2/sec

ρ = density of brine, 1.3 g/cm^3

ΔY = concentration difference across top layer Δx. Y is 100% saturated below Δx, and from the computer print-outs, Y is 99% saturated in the top element. Therefore, $\Delta Y = (1. - 0.99)0.263$ g/g.

q = salt flux. The flux by diffusion cannot exceed the amount of salt that can dissolve in the feed water. For 1 gal/hr feed, the salt that can dissolve is 1.68 kg/hr, or 0.47 g salt/sec.

r = cavity radius. Consider $r = 20 \times 10^2$ cm

Solving Equation 18:

$$\Delta x = D\ \Delta(\rho Y)\ \pi r^2/q = 1\ 04\ \text{cm}$$

This is not significant. But for longer times, diffusion becomes more important. When r is 100 x 10^2 cm, Δx = 26 cm. Or, when the feed rate is 1 gal/day and r = 20 x 10^2 cm, Δx = 25 cm. Therefore, at long times, diffusion will cause enough mixing of the top layer to increase the depth over which dissolving occurs.

Another effect that is likely more important than those already mentioned is the effect of a buildup of detritus from the dissolving salt in the top element. Typical rock salt contains 15 percent of insoluble material, in the form of anhydrite and fine clay-like particles. Solid layers of anhydrite are also common in bedded salt; these can range from paper-thin to a few cm in a layer of salt 50 cm deep. As the salt dissolves, these insolubles break off and fall down the cavity wall. In the Detroit cavity, where the wall sloped 10 or 20 degrees from the vertical, the detritus formed a layer 1 or 2 cm thick in some places. This layer was not taken into account in our model calculations, because it did not appear to affect the results significantly. Apparently, this material was sufficiently porous so that dissolution could continue with little change. If the growth is limited to the top element, then a shelf will form upon which this detritus can deposit, and it is certain to decrease the circulation of brine in this top element. The net result would be a reduction of dissolution in the top element, and the carrying down of unsaturated brine to lower elements, which would then tend to dissolve, resulting in a more gently-flaring cavity shape. Without some data on the permeability of such detritus layers, there is no way to estimate the importance of this effect. Such data could be obtained under field conditions, for example by a slow-flow experiment over a period of several months at the site of the Detroit cavity experiment.

Until the results of the model calculations were obtained, the importance of detritus in determining the detailed shape of the top layer was not recognized. If it is important to determine this more precisely, then further investigations of the effect of detritus on the dissolving rate would be required. At the present time, a 50-cm dissolving depth represents our best judgement of the effects that determine the dissolving depth.

7. GENERAL CONCLUSIONS

The objective of this project was to predict the growth of a cavity under very low flow rate of water entering the top of the cavity, and leaving from the bottom. This can occur in the case of a borehole connecting two aquifers. Model calculations calibrated by data from the Detroit Mine experiment show that with a low flow rate (1 gal/day) the brine in the cavity becomes saturated within a few thousand hours, except at the top where fresh water enters. For this reason dissolving occurs only in the top layer, and a wide-flaring cavity forms.

The depth of the top element in which dissolving occurs cannot be quantitatively predicted by the present model, because it depends on such effects as the covering of the surface of the salt by detritus.

Modification of the model to include the effects of detritus and further experiments to calibrate the modification would be needed to predict the details of the shape of the flaring top at long dissolving times. Based on our understanding of the relative importance of the various effects that can occur, we estimate that a 50-cm depth of the top dissolving layer is reasonable. From this assumption we can calculate the top layer diameter at any time and for any feed rate, since the volume of the top layer will increase to supply enough salt to saturate the quantity of water fed to the cavity. For example, at 1 gal/hr. the cavity diameter will grow to 208 m in 10,000 yrs. It will also grow to 657 m in 100,000 yr, but it seems unlikely that the influent rate will remain constant over such a long time.

The significance of this result is that a repository should be located at least 657 m from any existing borehole, to prevent the cavity from reaching the access shaft or altering the salt strata overlying the repository. On the other hand if the repository is located more than a few m below the top of the salt bed, the cavity can overlie the repository without reaching it. At these low flow rates the lower portion of the cavity grows very slowly (less than 1% as fast as the top layer).

8. FUTURE WORK

Since the predicted cavity size (cross-section) depends directly on the total amount of water fed, the prediction of feed rate is very important.

If it is determined that more accurate prediction of cavity shape over long time is desirable, then the variables affecting growth of the top layers should be further investigated. These variables were discussed above. Particularly important is the effect of detritus on the solution rate when the salt face becomes wide-flaring. The rate could be measured by laboratory simulation, followed by modification of the mathematical model, and eventual field calibration. A term for diffusion at long time could also be added to the model.

It seems likely that the inflow of water to the cavity will decrease to zero at some long time. Then the cavity growth process will stop as predicted by the present model. One should then consider whether there are other mechanisms that can cause further cavity growth, or change of shape. The thermal gradient that exists in the earth is one such mechanism. This gradient varies, but is about 1°F per 100 ft. This will cause the lower part of the cavity to be warmer than the top, and hence the brine along the lower walls will be warmer and less dense. This will cause an unstable convection, and a weak boundary layer flow up the cavity walls. Dissolution will occur along the walls, tending to equalize the brine density. When the more concentrated brine reaches the top, it will precipitate salt crystals. This effect is a very small one, and it has not been detected in any cavity where fresh water is being fed. It could only be significant at very long periods of time, such as 100,000 yr. An investigation could be proposed to estimate its importance.

At the present time other concepts are being considered for the storage of nuclear waste in salt, in place of the concept upon which this report is based. For this reason more detailed studies of the growth of cavities around boreholes may not be desired at the present time. It is hoped that the results of the present study will serve to evaluate any problems of cavity growth around boreholes that may need to be considered in the nuclear waste repository program.

REFERENCES

Nolen, J.S., Meister, S., Hieblinger, J., von Hantelmann, G., and Kleinitz, W., "Numerical Simulation of the Solution Mining Process," Paper 46d, AIChE Meeting, Tulsa, March 1974.

Saberian, Ahmed, 1974, "Numerical Simulation of Development of Solution-Mined Salt Cavities," Report for Solution Mining Research Institute.

Solution Mining Research Institute, 1969, "First Salt Cavity Experiment," Report of the SMRI, Chicago.

Snow, R.H., and Nielsen, H.J., 1970, IITRI-SMRI Solution Mining Studies, Third Symposium on Salt, J.T. Rau and L.F. Delwig, Eds., N. Ohio Geological Society, Cleveland, Ohio, pp. 341-359.

Table 1

Comparison of Computer Model with

Detroit Cavity Data Phase I

Parameter Values from Previous Regression Calculations

B'	b	C'	c	K_c'
1.00	300	.50	1.00	.0067

Time 14 Hr

Depth meter	Radius meter	Regression Rate cm/hr	Bulk Conc. Calc. % Satur.	Bulk Conc. Exp.	Flow kg/sec	Velocity cm/sec	DYDT 1/hr	DSalt g/sec	Density g/cm^3	SOLN g/cm-sec	DRAD g/sec	DRHO g/sec	BLFLOW g/sec	H cm
Influent Conc.		0.	Influent Rate		5.033									
1.0	1.005	1.415	4.0	2.0	4.875	.155	.000	26.716	1.008	.536	12.490	.028	157.644	1.99
2.0	.972	1.331	7.8	10.0	4.869	.162	.000	24.222	1.015	.488	11.466	.042	143.766	2.05
3.0	.937	1.259	11.1	12.0	4.902	.174	.000	21.986	1.023	.445	10.526	.046	131.182	2.07
4.0	.920	1.193	14.2	14.0	4.911	.179	.000	20.378	1.029	.414	9.865	.050	122.224	2.11
5.0	.912	1.132	17.1	18.0	4.918	.182	.000	19.096	1.035	.390	9.335	.054	115.038	2.14
6.0	.904	1.076	19.9	19.0	4.922	.184	.000	18.709	1.041	.367	8.637	.057	110.135	2.18
		Effluent Flow Rate			4.922									

Total Salt Produced up to this time 11062.42 kg

Accumulation of Salt in Sol. 511.82 kg

Total Salt Dissolved up to this time 36627.34 kg

Time 21 Hr

Depth meter	Radius meter	Regression Rate cm/hr	Bulk Conc. Calc. % Satur.	Bulk Conc. Exp.	Flow kg/sec	Velocity cm/sec	DYDT 1/hr	DSalt g/sec	Density g/cm^3	SOLN g/cm-sec	DRAD g/sec	DRHO g/sec	BLFLOW g/sec	H cm
Influent Conc.		0.	Influent Rate		0.									
1.0	1.102	1.208	13.5	11.0	-.186	-.005	.046	24.671	1.028	.503	11.909	19.414	146.995	2.10
2.0	1.065	1.131	17.2	16.0	-.208	-.006	.044	22.172	1.035	.454	10.836	17.462	132.947	2.15
3.0	1.023	1.065	20.6	21.0	-.226	-.007	.043	19.965	1.043	.411	9.869	15.741	120.438	2.19
4.0	1.002	1.005	23.5	23.0	-.249	-.006	.041	18.394	1.049	.380	9.189	14.491	111.635	2.23
5.0	.990	.952	26.2	27.0	-.264	-.008	.039	17.151	1.054	.356	8.646	13.522	104.539	2.27
6.0	.977	.896	29.1	33.0	-.290	-.009	.040	16.646	1.061	.331	8.084	13.264	96.076	2.32
		Effluent Flow Rate			-.290									

Total Salt Produced up to this time 17292.35 kg

Accumulation of Salt in Sol. 1132.45 kg

Total Salt Dissolved up to this time 43590.69 kg

Table 1 (cont'd)

Time 24.45 Hr

Depth meter	Radius meter	Regres-sion Rate cm/hr	Bulk Conc. Calc. % Satur.	Exp.	Flow kg/sec	Velocity cm/sec	DYDT 1/hr	DSalt g/sec	Density g/cm³	SOL. g/cm -sec	DRAD g/sec	DRHO g/sec	BLFLOW g/sec	H cm
Influent Conc.		0.	Influent Rate		0.									
1.0	1.129	.538	49.4	45.[illegible]	[illegible]	-.002	.017	10.[illegible]69	1.164	.229	5.820	7.787	66.724	2.75
2.0	1.088	.501	51.7	5[illegible]	-.091	-.002	.017	9.540	1.109	.206	5.246	6.973	59.920	2.82
3.0	1.047	.467	53.9	52.[illegible]	-.097	-.003	.016	8.515	1.113	.184	4.718	6.236	55.924	2.89
4.0	1.024	.444	55.5	55.0	-.105	-.003	.016	7.891	1.116	.172	4.402	5.752	50.516	2.95
5.0	1.011	.423	56.6	59.	-.114	-.003	.015	7.419	1.119	.161	4.153	5.411	47.401	2.98
6.0	.997	.376	[illegible]	62.0	-.119	-.003	.015	6.916	1.126	.142	3.661	5.322	42.164	3.10
		Effluent Flow Rate			-.119									

Total Salt Produced up to this time 17927.00 kg

Accumulation of Salt in Sol. 5525.55 kg

Total Salt Dissolved up to this time 45584.06 kg

Time 31 Hr

Depth meter	Radius meter	Regres-sion Rate cm/hr	Bulk Conc. Calc. % Satur.	Exp.	Flow kg/sec	Velocity cm/sec	DYDT 1/hr	DSalt g/sec	Density g/cm³	SOLN g/cm -sec	DRAD g/sec	DRHO g/sec	BLFLOW g/sec	H cm
Influent Conc.		0.	Influent Rate		0.									
1.0	1.150	.196	[illegible]	76.	-.05[illegible]	-.001	.006	3.867	1.156	.085	2.267	2.641	24.696	3.85
2.0	1.107	.181	75.1	73.[illegible]	-.032	-.001	.005	3.370	1.159	.070	2.016	2.349	21.949	3.96
3.0	1.065	.180	75.7	75.[illegible]	-.034	-.001	.005	2.986	1.151	.067	1.788	2.077	19.590	4.07
4.0	1.041	.159	77.[illegible]	76.[illegible]	-.037	-.001	.005	2.774	1.163	.062	1.672	1.925	18.550	4.13
5.0	1.027	.152	78.[illegible]	[illegible]	-.040	-.001	.005	2.513	1.164	.059	1.579	1.814	17.547	4.19
6.0	1.011	.121	81.1	[illegible]	-.034	-.001	[illegible]	2.274	1.171	.040	1.244	1.685	15.789	4.52
		Effluent Flow Rate			-.039									

Total Salt Produced up to this time 10726.55 kg

Accumulation of Salt in Sol. 5114.42 kg

Total Salt Dissolved up to this time 47155.07 kg

Table 2

Comparison of Computer Model with

Detroit Cavity Data Phase II

Parameter Values from Previous Regression Calculations

B'	b	C'	c	K_c'
0.578	200.	0.10	0.50	0.0048

Time 15 Hr

Depth meter	Radius meter	Regression Rate cm/hr	Bulk Conc. Calc. % Satur.	Bulk Conc. Exp. % Satur.	Flow kg/sec	Velocity cm/sec	DYDT 1/hr	DSalt g/sec	Density g/cm³	SOLN g/cm-sec	DRAD g/sec	DRHO g/sec	BLFLOW g/sec	H cm
Influent Conc:	0.	Influent Rate			.473									
1.0	1.836	.563	35.0	41.0	.316	.003	.000	18.878	1.073	.390	9.661	.193	157.311	2.07
2.0	1.685	.337	53.7	60.0	.366	.004	.000	10.087	1.113	.215	5.521	.138	106.672	2.14
3.0	1.574	.224	64.7	66.0	.395	.004	.000	6.125	1.136	.133	3.493	.097	77.755	2.20
4.0	1.467	.159	71.8	70.0	.413	.005	.000	4.010	1.151	.088	2.349	.057	58.880	2.25
5.0	1.362	.119	76.7	75.0	.423	.006	.000	2.888	1.161	.061	1.640	.015	49.647	2.29
		Effluent Flow Rate			.423									

Total Salt Produced up to this time 3130.21 kg

Accumulation of Salt in Sol. 6617.97 kg

Total Salt Dissolved up to this time 90158.47 kg

Time 76 Hr

Depth meter	Radius meter	Regression Rate cm/hr	Bulk Conc. Calc. % Satur	Bulk Conc. Exp. % Satur	Flow kg/sec	Velocity cm/sec	DYDT 1/hr	DSalt g/sec	Density g/cm³	SOLN g/cm-sec	DRAD g/sec	DRHO g/sec	BLFLOW g/sec	H cm
Influent Conc.	0.	Influent Rate			.473									
1.0	2.155	.514	38.8	43.0	.302	.002	.000	20.203	1.081	.416	10.433	.209	171.285	2.08
2.0	1.873	.297	57.4	64.0	.368	.003	.000	9.837	1.121	.210	5.443	.119	108.370	2.15
3.0	1.697	.195	67.8	70.0	.396	.004	.000	5.720	1.143	.125	3.294	.065	76.266	2.22
4.0	1.554	.138	74.3	78.0	.416	.005	.000	3.667	1.156	.081	2.166	.034	56.716	2.27
5.0	1.427	.103	78.8	84.0	.425	.006	.000	2.618	1.166	.055	1.496	.013	47.325	2.31
		Effluent Flow Rate			.425									

Total Salt Produced up to this time 21718.27 kg

Accumulation of Salt in Sol. 8485.87 kg

Total Salt Dissolved up to this time 112464.92 kg

Table 2 (cont'd)

Time 121 Hr

Depth meter	Radius meter	Regression Rate cm/hr	Bulk Conc. % Satur. Calc.	Bulk Conc. % Satur. Exp.	Flow kg/sec	Velocity cm/sec	DYDT 1/hr	DSalt g/sec	Density g/cm³	SOLN g/cm-sec	DRAD g/sec	DRHO g/sec	BLFLOW g/sec	H cm
Influent Conc.		0.	Influent Rate		.631									
1.0	2.400	.561	35.1	38.0	.423	.002	.000	24.669	1.073	.506	12.595	.258	207.459	2.07
2.0	2.072	.389	52.7	56.0	.498	.003	.000	12.530	1.111	.266	6.327	.171	132.704	2.13
3.0	1.799	.242	62.9	63.0	.535	.005	.000	7.575	1.132	.164	4.292	.107	94.635	2.18
4.0	1.629	.179	69.5	68.0	.558	.006	.000	5.028	1.146	.110	2.922	.066	71.682	2.23
5.0	1.485	.139	74.2	76.0	.570	.007	.000	3.697	1.156	.078	2.083	.037	60.129	2.27
		Effluent Flow Rate			.570									

Total Salt Produced up to this time 38606.46 kg

Accumulation of Salt in Sol. 8936.64 kg

Total Salt Dissolved up to this time 132206.92 kg

Time 176 Hr

Depth meter	Radius meter	Regression Rate cm/hr	Bulk Conc. % Satur. Calc.	Bulk Conc. % Satur. Exp.	Flow kg/sec	Velocity cm/sec	DYDT 1/hr	DSalt g/sec	Density g/cm³	SOLN g/cm-sec	DRAD g/sec	DRHO g/sec	BLFLOW g/sec	H cm
Influent Conc.		0.	Influent Rate		.316									
1.0	2.645	.346	52.9	56.0	.165	.001	.000	16.596	1.111	.346	8.679	.324	150.026	2.13
2.0	2.162	.166	71.1	71.0	.232	.001	.000	6.236	1.149	.135	5.595	.287	81.904	2.24
3.0	1.893	.099	79.3	82.0	.260	.002	.000	3.205	1.167	.071	1.917	.260	53.516	2.32
4.0	1.698	.068	83.9	85.0	.275	.003	.000	1.936	1.177	.045	1.182	.216	38.279	2.38
5.0	1.536	.049	86.9	84.0	.282	.003	.000	1.341	1.183	.029	.786	.163	31.291	2.43
		Effluent Flow Rate			.282									

Total Salt Produced up to this time 53862.73 kg

Accumulation of Salt in Sol. 13881.63 kg

Total Salt Dissolved up to this time 153451.53 kg

Table 3

PREDICTION OF CAVITY GROWTH AT FEED RATE 1 gal/hr

Time 50 Hr — Feed Rate = 72 gal/min

Depth meter	Radius meter	Regression Rate cm/hr	Bulk Conc. Calc. % Satur.	Exp.	Flow kg/sec	Velocity cm/sec	DYDT 1/hr	DSalt g/sec	Density g/cm³	SOLN g/cm-sec	DRAD g/sec	DRHO g/sec	BLFLOW g/sec	H cm
INFLUENT CONC		.00000	INFLUENT RATE		.45166+01									
0.5	1.5486	.1431+01	3.3	.0	.430+01	.568-01	.759-04	.398+02	1.005	.836	19.424	.06	242.674	1.918
1.0	1.5099	.1361+01	6.5	.0	.433+01	.598-01	.115-03	.382+02	1.011	.776	18.133	.09	225.441	1.953
1.5	1.4718	.1298+01	9.4	.0	.437+01	.631-01	.144-03	.352+02	1.017	.721	16.958	.11	209.889	1.987
2.0	1.4382	.1240+01	12.1	.0	.440+01	.662-01	.166-03	.327+02	1.023	.673	15.927	.12	196.310	2.021
2.5	1.4038	.1188+01	14.6	.0	.443+01	.696-01	.182-03	.303+02	1.028	.630	14.966	.12	183.780	2.052
3.0	1.3708	.1140+01	16.9	.0	.446+01	.731-01	.19[illegible]-03	.283+02	1.033	.590	14.093	.13	172.437	2.083
3.5	1.3441	.1096+01	19.1	.0	.448+01	.761-01	.202-03	.265+02	1.038	.556	13.343	.13	162.694	2.113
4.0	1.3259	.1055+01	21.1	.0	.450+01	.782-01	.208-03	.250+02	1.042	.528	12.723	.13	154.633	2.141
4.5	1.3087	.1017+01	23.0	.0	.452+01	.803-01	.213-03	.236+02	1.046	.503	12.151	.13	147.224	2.169
5.0	1.2923	.9817+00	24.8	.0	.454+01	.824-01	.216-03	.224+02	1.050	.479	11.621	.13	140.395	2.197
5.5	1.2768	.9484+00	26.5	.0	.456+01	.845-01	.217-03	.213+02	1.053	.457	11.130	.12	133.948	2.221
6.0	1.2614	.9157+00	28.2	.0	.457+01	.866-01	.218-03	.212+02	1.057	.436	10.652	.12	130.796	2.301
EFFLUENT FLOW RATE					.457+01									

TOTAL OF SALT PRODUCED IN KG .51146114+05 — TOTAL OF SALT ACCUMULATED IN CAVITY IN KG .15860434+04 — TOTAL OF SALT DISSOLVED IN KG .77902680+05

Time 20.8 days — Feed Rate = 10 gal/min

Depth meter	Radius meter	Regression Rate cm/hr	Bulk Conc. Calc. % Satur.	Exp.	Flow kg/sec	Velocity cm/sec	DYDT 1/hr	DSalt g/sec	Density g/cm³	SOLN g/cm-sec	DRAD g/sec	DRHO g/sec	BLFLOW g/sec	H cm
INFLUENT CONC		.00000	INFLUENT RATE		.62997+00									
0.5	7.4599	.1220+01	13.3	.0	-.301+00	-.168-03	.556-02	.159+03	1.025	3.435	81.405	*****	913.205	1.853
1.0	6.7491	.1018+01	23.2	.0	-.105+00	-.700-04	.518-02	.123+03	1.046	2.592	62.681	82.31	701.891	2.005
1.5	6.1866	.8726+00	30.7	.0	.272-01	.213-04	.470-02	.945+02	1.062	2.037	50.005	62.67	559.105	2.139
2.0	5.7305	.7635+00	36.6	.0	.120+00	.109-03	.433-02	.753+02	1.078	1.651	41.003	49.51	457.950	2.260
2.5	5.3478	.6786+00	41.4	.0	.189+00	.194-03	.403-02	.615+02	1.088	1.370	34.331	40.22	383.082	2.370
3.0	5.0222	.6108+00	45.4	.0	.242+00	.279-03	.380-02	.514+02	1.093	1.158	29.242	33.41	325.939	2.471
3.5	4.7455	.5553+00	48.7	.0	.282+00	.363-03	.360-02	.437+02	1.100	.995	25.283	28.27	281.535	2.565
4.0	4.5105	.5090+00	51.6	.0	.314+00	.444-03	.343-02	.377+02	1.106	.866	22.150	24.32	246.417	2.653
4.5	4.3032	.4698+00	54.1	.0	.340+00	.526-03	.328-02	.329+02	1.111	.763	19.598	21.17	217.841	2.735
5.0	4.1187	.4362+00	56.3	.0	.361+00	.608-03	.315-02	.291+02	1.116	.678	17.489	18.63	194.236	2.813
5.5	3.9533	.4070+00	58.3	.0	.380+00	.691-03	.304-02	.259+02	1.120	.607	15.723	16.54	173.996	2.879
6.0	3.7950	.3799+00	60.2	.0	.388+00	.762-03	.313-02	.247+02	1.124	.544	14.100	15.72	163.272	3.085
EFFLUENT FLOW RATE					.388+00									

TOTAL OF SALT PRODUCED IN KG .10187267+07 — TOTAL OF SALT ACCUMULATED IN CAVITY IN KG .55696974+05 — TOTAL OF SALT DISSOLVED IN KG .11368364+07

Table 3 (cont'd)

Time 208 days — Feed Rate = 1 gal/hr

Depth meter	Radius meter	Regres-sion Rate cm/hr	Bulk Conc. Calc. % Satur.	Bulk Conc. Exp. % Satur.	Flow kg/sec	Velocity cm/sec	DYDT 1/hr	DSalt g/sec	Density g/cm³	SOLN g/cm-sec	DRAD g/sec	DRHO g/sec	BLFLOW g/sec	H cm
INFLUENT CONC		.00000	INFLUENT RATE		.10520-02									
0.5	11.9585	.2016-02	98.8	.0	.115-02	.212-06	.806-07	.331+00	1.205	.009	.254	.00	.102	.659
1.0	8.7146	.1452-04	100.0	.0	.124-02	.432-06	.703-07	.665-02	1.208	.000	.001	.00	.006	23.202
1.5	7.3829	.0000	100.0	.0	.125-02	.603-06	.414-07	.130-02	1.208	.000	.000	.00	.000	.000
2.0	6.563[illegible]	.0000	100.0	.0	.125-02	.763-06	.324-07	.678-03	1.208	.000	.001	.00	.000	.000
2.5	5.9735	.0000	100.0	.0	.125-02	.922-06	.121-07	.269-03	1.208	.000	.000	.00	.000	.000
3.0	5.5162	.0000	100.0	.0	.125-02	.108-05	.260-07	.397-03	1.208	.000	.000	.00	.000	.000
3.5	5.1491	.0000	100.0	.0	.125-02	.124-05	.130-07	.206-03	1.208	.000	.000	.00	.000	.000
4.0	4.8488	.0000	100.0	.0	.125-02	.140-05	.238-07	.281-03	1.208	.000	.000	.00	.000	.000
4.5	4.5921	.0000	100.0	.0	.125-02	.156-05	.176-07	.205-03	1.208	.000	.000	.00	.000	.000
5.0	4.3691	.0000	100.0	.0	.125-02	.172-05	.193-07	.194-03	1.208	.000	.000	.00	.000	.000
5.5	4.1725	.0000	100.0	.0	.125-02	.189-05	.156-07	.150-03	1.208	.000	.000	.00	.000	.000
6.0	3.9828	.0000	100.0	.0	.125-02	.207-05	.876-08	.865-04	1.208	.000	.000	.00	.000	.000
EFFLUENT FLOW RATE					.125-02									

TOTAL OF SALT PRODUCED IN KG .13954304+07 — TOTAL OF SALT ACCUMULATED IN CAVITY IN KG .25160630+06 — TOTAL OF SALT DISSOLVED IN KG .17194070+07

Time 5.7 yrs — Feed Rate = 1 gal/hr

Depth meter	Radius meter	Regres-sion Rate cm/hr	Bulk Conc. Calc. % Satur.	Bulk Conc. Exp. % Satur.	Flow kg/sec	Velocity cm/sec	DYDT 1/hr	DSalt g/sec	Density g/cm³	SOLN g/cm-sec	DRAD g/sec	DRHO g/sec	BLFLOW g/sec	H cm
INFLUENT CONC		.00000	INFLUENT RATE		.10520-02									
0.5	12.8009	.1835-02	98.9	.0	.120-02	.193-06	.286-08	.325+00	1.205	.009	.247	.00	.052	.354
1.0	8.7170	.4969-05	100.0	.0	.125-02	.433-06	.492-10	.368-02	1.208	.000	.000	.00	.000	4.139
1.5	7.3829	.0000	100.0	.0	.125-02	.604-06	.435-12	.705-04	1.208	.000	.000	.00	.000	.000
2.0	6.5633	.0000	100.0	.0	.125-02	.764-06	.882-11	.115-05	1.208	.000	.000	.00	.000	.000
2.5	5.9735	.0000	100.0	.0	.125-02	.922-06	.145-10	.646-06	1.208	.000	.000	.00	.000	.000
3.0	5.5162	.0000	100.0	.0	.125-02	.108-05	.182-10	.454-06	1.208	.000	.000	.00	.000	.000
3.5	5.1491	.0000	100.0	.0	.125-02	.124-05	.192-10	.357-06	1.208	.000	.000	.00	.000	.000
4.0	4.8438	.0000	100.0	.0	.125-02	.140-05	.190-10	.295-06	1.208	.000	.000	.00	.000	.000
4.5	4.5921	.0000	100.0	.0	.125-02	.156-05	.171-10	.246-06	1.208	.000	.000	.00	.000	.000
5.0	4.3691	.0000	100.0	.0	.125-02	.172-05	.160-10	.208-06	1.208	.000	.000	.00	.000	.000
5.5	4.1725	.0000	100.0	.0	.125-02	.189-05	.155-10	.179-06	1.208	.000	.000	.00	.000	.000
6.0	3.9828	.0000	100.0	.0	.125-02	.207-05	.139-10	.153-06	1.208	.000	.000	.00	.000	.000
EFFLUENT FLOW RATE					.125-02									

TOTAL OF SALT PRODUCED IN KG .14479000+07 — TOTAL OF SALT ACCUMULATED IN CAVITY IN KG .26200242+06 — TOTAL OF SALT DISSOLVED IN KG .17900112+07

Table 3 (cont'd)

Time 3,424 yr   Feed Rate = 1 gal/hr

Depth meter	Radius meter	Regres-sion Rate cm/hr	Bulk Conc. Calc. % Satur.	Exp.	Flow kg/sec	Velocity cm/sec	DYDT 1/hr	DSalt g/sec	Density g/cm³	SOLN g/cm-sec	DRAD g/sec	DRHO g/sec	BLFLOW g/sec	H cm
Influent Conc. = 0.			Influent Rate =		.10520-02									
1.0	10.255	0.	100.[illegible]	[illegible]	.125-02	.314-06	.469-06	.268-01	1.208	0.	0.	.02	.007	19.753
2.0	6.579	0.	100.[illegible]	[illegible]	.125-02	.762-06	.260-09	.323-05	1.208	0.	0.	.00	.000	0.
3.0	5.520	0.	100.0	0.	.125-02	.108-05	-.385-11	.447-06	1.208	0.	0.	-.00	.000	0.
4.0	4.851	0.	100.0	0.	.125-02	.140-05	.492-12	.146-06	1.208	0.	0.	.00	.000	0.
5.0	4,371	0.	100.0	0.	.125-02	.173-05	.738-12	.681-07	1.208	0.	0.	.00	.000	C.
6.0	3.984	0.	100.0	0.	.125-02	.208-05	.667-12	.382-07	1.208	0.	0.	.00	.000	0.
		Effluent Flow Rate =			.125-02									

Total Salt Produced in this time .36873910+08 kg

Accumulation of Salt in Sol. .76818949+07 kg

Total Salt Dissolved up to this time .52430398+08 kg

Time 11,415 yr   Feed Rate = 1 gal/hr

Depth meter	Radius meter	Regres-sion Rate cm/hr	Bulk Conc. Calc. % Satur.	Exp.	Flow kg/sec	Velocity cm/sec	DYDT 1/hr	DSalt g/sec	Density g/cm³	SOLN g/cm-sec	DRAD g/sec	DRHO g/sec	BLFLOW g/sec	H cm
Influent Conc. = 0.			Influent Rate =		.10520-02									
0.5	222.775													
1.0	11.155	0.	100.0	0.	.125-02	.265-06	.412-06	.276-01	1.208	0.	0.	.02	0.	25.815
2.0	6.591	0.	100.0	0.	.125-02	.760-06	.141-09	.156-05	1.208	0.	0.	.00	0.	0.
3.0	5.522	0.	100.0	0.	.125-02	.108-05	.175-11	.275-06	1.208	0.	0.	.00	0.	0.
4.0	4.852	0.	100.0	0.	.125-02	.140-05	.905-12	.105-06	1.208	0.	0.	.00	0.	0.
5.0	4.371	0.	100.0	0.	.125-02	.173-05	.108-11	.529-07	1.208	0.	0.	.00	0.	0.
6.0	3.984	0.	100.0	0.	.125-02	.208-05	.992-12	.316-07	1.208	0.	0.	.00	0.	0.
		Effluent Flow Rate =			.125-02									

Total Salt Produced up to this time .11972462+09 kg

Accumulation of Salt in Sol. .24938368+08 kg

Total Salt Dissolved up to this time .17005115+09 kg

Table 4

PREDICTION OF CAVITY GROWTH AT FEED RATE 1 gal/day

Time 50 Hr — Feed Rate = 72 gal/min

Depth meter	Radius meter	Regression Rate cm/hr	Bulk Conc. % Satur. Calc.	Bulk Conc. % Satur. Exp.	Flow kg/sec	Velocity cm/sec	DYDT 1/hr	DSalt g/sec	Density g/cm³	SOLN g/cm-sec	DRAD g/sec	DRHO g/sec	BLFLOW g/sec	H cm
INFLUENT CONC		.00000	INFLUENT RATE		.45166+01									
0.5	1.5486	.1431+01	3.3	.0	.430+01	.568-01	.759-04	.398+02	1.005	.836	19.424	.06	242.674	1.918
1.0	1.5099	.1361+01	6.5	.0	.433+01	.598-01	.115-03	.382+02	1.011	.776	18.133	.09	225.441	1.953
1.5	1.4718	.1298+01	9.4	.0	.437+01	.631-01	.144-03	.352+02	1.017	.721	16.958	.11	209.889	1.987
2.0	1.4382	.1240+01	12.1	.0	.440+01	.662-01	.166-03	.327+02	1.023	.673	15.927	.12	196.310	2.021
2.5	1.4038	.1188+01	14.6	.0	.443+01	.696-01	.182-03	.303+02	1.028	.630	14.966	.12	183.780	2.052
3.0	1.3708	.1140+01	16.9	.0	.446+01	.731-01	.193-03	.283+02	1.033	.590	14.093	.13	172.437	2.083
3.5	1.3441	.1096+01	19.1	.0	.448+01	.761-01	.202-03	.265+02	1.038	.556	13.343	.13	162.694	2.113
4.0	1.3259	.1055+01	21.1	.0	.450+01	.782-01	.208-03	.250+02	1.042	.528	12.723	.13	154.633	2.141
4.5	1.3087	.1017+01	23.0	.0	.452+01	.803-01	.213-03	.236+02	1.046	.503	12.151	.13	147.224	2.169
5.0	1.2923	.9817+00	24.8	.0	.454+01	.824-01	.216-03	.224+02	1.050	.479	11.621	.13	140.395	2.197
5.5	1.2768	.9484+00	26.5	.0	.456+01	.845-01	.217-03	.213+02	1.053	.457	11.130	.12	133.048	2.221
6.0	1.2614	.9157+00	28.2	.0	.457+01	.866-01	.218-03	.212+02	1.057	.436	10.652	.12	130.796	2.301
EFFLUENT FLOW RATE					.457+01									

TOTAL OF SALT PRODUCED IN KG .51140114+05 TOTAL OF SALT ACCUMULATED IN CAVITY IN KG .15860434+04 TOTAL OF SALT DISSOLVED IN KG .77902680+05

Time 20.8 days — Feed Rate = 10 gal/min

Depth meter	Radius meter	Regression Rate cm/hr	Bulk Conc. % Satur Calc.	Bulk Conc. % Satur Exp.	Flow kg/sec	Velocity cm/sec	DYDT 1/hr	DSalt g/sec	Density g/cm³	SOLN g/cm-sec	DRAD g/sec	DRHO g/sec	BLFLOW g/sec	H cm
INFLUENT CONC		.00000	INFLUENT RATE		.62997+00									
0.5	7.4599	.1220+01	13.3	.0	-.301+00	-.168-03	.556-02	.159+03	1.025	3.435	81.405	*****	913.205	1.853
1.0	6.7491	.1018+01	23.2	.0	-.105+00	-.700-04	.518-02	.123+03	1.046	2.592	62.681	82.31	701.891	2.005
1.5	6.1866	.8726+00	30.7	.0	.272-01	.213-04	.470-02	.945+02	1.062	2.037	50.005	62.67	559.145	2.139
2.0	5.7305	.7635+00	36.6	.0	.120+00	.109-03	.433-02	.753+02	1.074	1.651	41.003	49.51	457.950	2.260
2.5	5.3478	.6786+00	41.4	.0	.189+00	.194-03	.403-02	.615+02	1.084	1.370	34.331	40.?2	383.042	2.370
3.0	5.0222	.6108+00	45.4	.0	.242+00	.279-03	.380-02	.514+02	1.093	1.158	29.242	33.41	325.939	2.471
3.5	4.7455	.5553+00	48.7	.0	.282+00	.363-03	.360-02	.437+02	1.100	.995	25.283	28.27	281.533	2.565
4.0	4.5105	.5090+00	51.6	.0	.314+00	.444-03	.343-02	.377+02	1.106	.866	22.150	24.32	246.417	2.653
4.5	4.3032	.4698+00	54.1	.0	.340+00	.526-03	.328-02	.329+02	1.111	.763	19.598	21.17	217.841	2.735
5.0	4.1187	.4362+00	56.3	.0	.361+00	.608-03	.315-02	.291+02	1.116	.678	17.489	18.63	194.236	2.813
5.5	3.9533	.4070+00	58.3	.0	.380+00	.691-03	.304-02	.259+02	1.120	.607	15.723	16.54	173.996	2.879
6.0	3.7959	.3799+00	60.2	.0	.388+00	.762-03	.313-02	.247+02	1.124	.544	14.140	15.72	163.272	3.085
EFFLUENT FLOW RATE					.388+00									

TOTAL OF SALT PRODUCED IN KG .10167267+07 TOTAL OF SALT ACCUMULATED IN CAVITY IN KG .55696974+05 TOTAL OF SALT DISSOLVED IN KG .11364364+07

Table 4 (cont'd)

Time 208 days Feed Rate = 1 gal/day

Depth meter	Radius meter	Regression Rate cm/hr	Bulk Conc. Calc. % Satur.	Exp.	Flow kg/sec	Velocity cm/sec	DYDT 1/hr	DSalt g/sec	Density g/cm³	SOLN g/cm-sec	DRAD g/sec	DRHO g/sec	BLFLOW g/sec	H cm
INFLUENT CONC		.00000	INFLUENT RATE		.43832-04									
0.5	11.9146	.2490-03	99.7	.0	.241-04	.448-08	.323-06	.379-01	1.207	.001	.031	.02	.028	3.006
1.0	8.7139	.0000	100.0	.0	.503-04	.175-07	.102-06	.411-02	1.208	.000	.001	.00	.000	.000
1.5	7.3828	.0000	100.0	.0	.503-04	.243-07	.570-08	.166-03	1.208	.000	.000	.00	.000	.000
2.0	6.5633	.0000	100.0	.0	.503-04	.308-07	.292-07	.660-03	1.208	.000	.001	.00	.000	.000
2.5	5.9734	.0000	100.0	.0	.503-04	.371-07	.118-07	.223-03	1.208	.000	.000	.00	.000	.000
3.0	5.5162	.0000	100.0	.0	.502-04	.435-07	.268-07	.429-03	1.208	.000	.000	.00	.000	.000
3.5	5.1491	.0000	100.0	.0	.502-04	.499-07	.140-07	.197-03	1.208	.000	.000	.00	.000	.000
4.0	4.8488	.0000	100.0	.0	.502-04	.563-07	.245-07	.303-03	1.208	.000	.000	.00	.000	.000
4.5	4.5921	.0000	100.0	.0	.502-04	.627-07	.170-07	.189-03	1.208	.000	.000	.00	.000	.000
5.0	4.3691	.0000	100.0	.0	.502-04	.693-07	.198-07	.199-03	1.208	.000	.000	.00	.000	.000
5.5	4.1725	.0000	100.0	.0	.502-04	.759-07	.151-07	.139-03	1.208	.000	.000	.00	.000	.000
6.0	3.9828	.0000	100.0	.0	.502-04	.833-07	.766-08	.647-04	1.208	.000	.000	.00	.000	.000
EFFLUENT FLOW RATE					.502-04									

TOTAL OF SALT PRODUCED IN KG .13920787+07 TOTAL OF SALT ACCUMULATED IN CAVITY IN KG .25185197+06 TOTAL OF SALT DISSOLVED IN KG .17157961+07

Time 5.7 yrs Feed Rate = 1 gal/day

Depth meter	Radius meter	Regression Rate cm/hr	Bulk Conc. Calc. % Satur.	Exp.	Flow kg/sec	Velocity cm/sec	DYDT 1/hr	DSalt g/sec	Density g/cm³	SOLN g/cm-sec	DRAD g/sec	DRHO g/sec	BLFLOW g/sec	H cm
INFLUENT CONC		.00000	INFLUENT RATE		.43832-04									
0.5	11.9532	.8233-04	99.9	.0	.519-04	.958-08	.185-10	.137-01	1.208	.000	.010	.00	.000	.052
1.0	8.7139	.0000	100.0	.0	.520-04	.181-07	.282-11	.198-04	1.208	.000	.000	.00	.000	.000
1.5	7.3828	.0000	100.0	.0	.520-04	.252-07	.320-10	.896-06	1.208	.000	.000	.00	.000	.000
2.0	6.5633	.0000	100.0	.0	.520-04	.318-07	.330-10	.750-06	1.208	.000	.000	.00	.000	.000
2.5	5.9734	.0000	100.0	.0	.520-04	.384-07	.262-10	.500-06	1.208	.000	.000	.00	.000	.000
3.0	5.5162	.0000	100.0	.0	.520-04	.451-07	.243-10	.394-06	1.208	.000	.000	.00	.000	.000
3.5	5.1491	.0000	100.0	.0	.520-04	.517-07	.210-10	.298-06	1.208	.000	.000	.00	.000	.000
4.0	4.8488	.0000	100.0	.0	.520-04	.583-07	.196-10	.245-06	1.208	.000	.000	.00	.000	.000
4.5	4.5921	.0000	100.0	.0	.520-04	.650-07	.175-10	.197-06	1.208	.000	.000	.00	.000	.000
5.0	4.3691	.0000	100.0	.0	.520-04	.718-07	.166-10	.168-06	1.208	.000	.000	.00	.000	.000
5.5	4.1725	.0000	100.0	.0	.520-04	.768-07	.151-10	.141-06	1.208	.000	.000	.00	.000	.000
6.0	3.9828	.0000	100.0	.0	.520-04	.865-07	.131-10	.112-06	1.208	.000	.000	.00	.000	.000
EFFLUENT FLOW RATE					.520-04									

TOTAL OF SALT PRODUCED IN KG .13942621+07 TOTAL OF SALT ACCUMULATED IN CAVITY IN KG .25248044+06 TOTAL OF SALT DISSOLVED IN KG .17189221+07

Appendix

LISTING OF COMPUTER PROGRAM

```
      DIMENSION    FLUX(50), DSALT(50), DYDT(50), Y(50),
     1               A(5), R(50), RHOI(50), REGRES(50)
      DIMENSION    SOLN(50), DRAD(50), TIMPR(50), QCHANG(50),
     1             RS(50), YS(50), H(50), BLFLOW(50), DRHO(50),
     2             TFLOW(50), Z(10), SUBT(50)
      LOGICAL*1    ENDCAS , OUTPUT
 1000 FORMAT('1', ' THE PREDICTION OF CAVITY GROTH')
 1005 FORMAT('0',2X,'NX',5X,'HT',5X,'NT',2X,'QFEED(CC/S)',6X,
     1             'TEMP(OC)',8X,'KCP',7X,'AX',1X,'TINC',2X,'STEPS' )
 1009 FORMAT( )
 1010 FORMAT('0', I5, F10.2, I5, 2F15.2, F10.5, 2F5.1, I5 )
 1013 FORMAT( 3 I5 )
 1015 FORMAT('0', ' TIME TO PRINT IN HOURS' )
 1017 FORMAT( 6F10.2 )
 1020 FORMAT(' ', 10E10.4 )
 1023 FORMAT('0', ' TIMES TO CHANGE FLOW' )
 1024 FORMAT(' ', ' TIME', 5X, ' FLOW CHANGED' )
 1022 FORMAT( )
 1025 FORMAT('0', 3X, ' RADIUS(CM)', 2X, ' Y(G/G) ' )
 1030 FORMAT(' ', F10.3, F15.7 )
 1035 FORMAT('0', 6X, ' COEFFICIENTS FOR BLFLOW' )
 1040 FORMAT(' ', '      BPR         CPR          BEXP          CEXP       KCP')
 1045 FORMAT( 5E10.3 )
 1050 FORMAT('1' )
 1055 FORMAT('0','TIME=', E10.3,25X,'NO. OF ITERATION IS',I10,5X,
     1             'FLOW RATE IS', 2X, E7.3, 2X, 'GALLONS/M' )
 1060 FORMAT('0', 'DEPTH',4X,'RADIUS',4X,'REGRES',3X,'CALC',3X,'EXPT',
     1             5X,'FLOW',4X,'VELOC.',5X,'DYDT',4X,'DSALT',
     2             1X,'DENSITY',3X,'SOLN',4X,'DRAD',4X,'DRHO',
     3             2X,'BLFLOW', 5X, 'H' )
 1065 FORMAT(' ', 'METER', 4X, 'METER', 5X,'CM/HR',3X,'% SATUR.',
     1             1X, '% SAT.', 2X,
     1                  'KG/SEC',2X,'CM/SEC',5X,'/HR',5X,'G/SEC',
     2             1X,'G/CM3',3X,'G/CM-SEC',2X,'G/SEC' )
 1070 FORMAT('0', 'INFLUENT CONC', F10.5,2X,  'INFLUENT RATE', E12.5 )
 1075 FORMAT(' ', F5.1, F10.4, E10.4, 2F7.1, 4E9.3, 2F7.3 ,
     1             2X, F8.3, 3X, F5.2, 2F8.3 )
 1080 FORMAT(' ', ' EFFLUENT FLOW RATE', 20X, E9.3 )
 1085 FORMAT('0', 'TOTAL OF SALT PRODUCED IN KG',5X,
     1             'TOTAL OF SALT ACCUMULATED IN CAVITY IN KG',20X,
     2             'TOTAL OF SALT DISSOLVED IN KG' )
 1090 FORMAT(' ', 10X, E15.8, 25X, E15.8, 36X, E15.8 )
C
C ********     STANDARD INPUT DATA
C
      WRITE(6,1000 )
      WRITE(6, 1005 )
      READ(5, 1009) NX, HT, NT, QFEED, TEMP, CKCP, AX, TINC, NDX
      WRITE(6,1010) NX, HT, NT, QFEED, TEMP, CKCP, AX, TINC, NDX
      READ(5,1013) ITPR, KTF, NEXP
      WRITE(6,1015)
      READ(5,1022) ( TIMPR(I), I=1,ITPR )
        DO 10 I=1, ITPR
             SUBT(I) = TIMPR(I)
   10        TIMPR(I) = TIMPR(I)*3600.
      WRITE(6,1020)(  SUBT(I), I=1,ITPR )
```

```
          WRITE(6,1023)
          WRITE(6,1024)
             DO 13 I= 1, KTF
          READ(5,1030) ( TFLOW(I), QCHANG(I) )
          WRITE(6,1030)( TFLOW(I), QCHANG(I) )
                   TFLOW(I) = TFLOW(I)*3600.
       13 CONTINUE
                   TF= 32. + TEMP*1.8
                   QFEE = QFEED*16.6666
                   DX= HT/NX
                   NT = NT*100
                   PI= 3.14159
                   YFEED= 0.
                   RHOW= 1.
                   RHOS= 2.1654- .00012*TEMP
                   ALFA= .806 - 9.63E-05*TF
                   RHOF= RHOW + ALFA*YFEED
                   YY= .3568 + .00001*TF*( .0085*TF - .175 )
                   YSTAR= YY/( 1. + YY )
                   NNX = NX + 1
          WRITE(6,1025)
    C
    C********      TAKE AVERAGE OF NTH AND N-1TH DEPTH TO BE CELL'S
    C              RADIUS AND CONCENTRATION
             DO 15 IX= 1, NNX
          READ(5,1030) ( R(IX), Y(IX) )
                   R(IX) = R(IX)*100.
                   RS(IX) = R(IX)
                   YS(IX) = Y(IX)
       15 CONTINUE
             DO 20 IX=2, NNX
                   JX= IX-1
                   R(JX)=( RS(IX) + RS(JX) )/2.
                   Y(JX)= ( YS(IX) + YS(JX) )/ 2.
                   FLUX(JX) = QFEED*RHOF
          WRITE(6,1030) ( R(JX), Y(JX) )
       20 CONTINUE
             DO 18 JX = 1, NX
                   RS(JX) = R(JX)
                   YS(JX) = Y(JX)
       18 CONTINUE
          WRITE(6,1035)
          WRITE(6,1040)
          READ(5,1045) ( A(I), I = 1, 5 )
          WRITE(6,1045)( A(I), I = 1, 5 )
          WRITE(6,1050 )
    C
    C*********      INITIALIZATION
    C
       50 CONTINUE
                   DI = 60.
                   ENDCAS = .FALSE.
                   OUTPUT= .FALSE.
                   TIME= 0.
                   DSALT(1) =0.
                   REMOV = 0.
                   NCOUNT = 1
```

```
                  NPR = 0
                  JEXP = 1
                  SIGMA = .0001
                  KKK = 1
                  MMM = 1
                        NNN = 0
                  KX = 0
                  QFEED = QFEE
                  TEMP6 = 45.*3600.
            DO 80 J=1, NX
                  R(J) = RS(J)
                  Y(J) = YS(J)
   80 CONTINUE
C
C*********     ITERATION WITH INCREMENT OF TIME
C
   90       DO 500 IT = 1, NT
                  DT1 = DT
                  TIME = TIME + DT
          IF( MMM .GT. KTF ) GO TO 100
          IF( TIME .LT. TFLOW(MMM) ) GO TO 100
                  QFEED = QCHANG(MMM)*16.666
                  MMM = MMM + 1
  100     IF( KKK .GT. ITPR ) GO TO 600
          IF( TIME .LT. TIMPR(KKK) ) GO TO 102
                  DT = TIME - TIMPR(KKK)
                  TIME = TIMPR(KKK )
                  OUTPUT = .TRUE.
                  KKK = KKK + 1
C
C*********     CONSIDERATION OF MIXING FACTOR ON TOP
C
  102             FEED = QFEED*RHOF
                  Y2 = ( Y(2)-Y(1) )*AX*FEED
          IF( TIME .GT. TEMP6 ) Y2 = 0.
                  RLOSS = 0.
                  DISS = 0.
                  ACCUM = 0.
                  UMAX = MIN( .01, 1500./TIME )
                  Y3 = -Y2
C
C*********     CALCULATIONS ALONG WITH INCREMENT OF DEPTH
C
            DO 300 IX = 1, NX
                  RHOI(IX) = 1.-4.8E-07*TF**2.+ALFA*Y(IX)
                  S1 = YSTAR - Y(IX)
          IF( S1 .GT. 0. ) GO TO 108
                  S1 = 0.
                  S2 = 0.
                  H(IX) = 0.
                  BLFLOW(IX) = 0.
          GO TO 109
  108             K1 = IX + 1
          IF( IX .EQ. NX ) K1 = NX
                  S3 = 1. - ( Y(K1)-Y(IX) )/S1
                  SKC = A(5)*S1**.5
                  S2 = SKC*S1
```

```
                     H(IX) = 1./( A(1)*S1**A(3) )*S3
          IF ( H(IX) .LT. DX ) GO TO 105
                     H(IX) = 0.
                     BLFLOW(IX) = 0.
          GO TO 109
      105 CONTINUE
                     BLFLOW(IX) = 2.*A(2)*PI*R(IX)*S3*SKC*S1**A(4)
      109            REGRES(IX) = S2/RHOS
                     SOLN(IX) = 2.*PI*R(IX)*S2
                     DRAD(IX) = SOLN(IX)*RHOI(IX)*DX/RHOS
                     S4 = Y(IX) - YSTAR
      110            TEMP0 = FLUX(IX)
                     TEMP1 = SOLN(IX)*( 1.-Y(IX) )*DX
          IF( IX .GT. 1 ) GO TO 115
                     DSALT(IX) = TEMP1 - SOLN(IX)*H(IX)
                     DYT=DSALT(IX)+FLUX(IX)*(YFEED-Y(IX)) -BLFLOW(IX)*Y(IX)
              GO TO 155
      115            TEMP2 =( FLUX(IX)+BLFLOW(IX) )*(Y(IX-1) - Y(IX) )
DIAGNOSTIC*  THE TEST FOR EQUALITY BETWEEN NON-INTEGERS MAY NOT BE MEANINGFUL.
          IF( H(IX-1 ) .EQ. 0. ) H(IX) = 0.
DIAGNOSTIC*  THE TEST FOR EQUALITY BETWEEN NON-INTEGERS MAY NOT BE MEANINGFUL.
          IF( H(IX) .EQ. 0. ) REGRES(IX) = 0.
          IF( IX .EQ. NX ) GO TO 120
                     DSALT(IX)= TEMP1+ SOLN(IX-1)*H(IX-1)-SOLN(IX)*H(IX)
          GO TO 150
      120            DSALT(IX)= TEMP1 + SOLN(IX-1)*H(IX-1)
      150            DYT= DSALT(IX) + TEMP2
      155            TEMP3 = PI*R(IX)**2.*DX
                     DYDT(IX) = ( DYT+Y2 )/(TEMP3*RHOI(IX) )
          IF( IX .GT. 1 ) GO TO 160
                     TEMP4 = FEED - BLFLOW(IX)
          GO TO 170
      160            TEMP4 = FLUX(IX-1) + BLFLOW(IX-1) - BLFLOW(IX)
      170            FLUX(IX) = TEMP4 - DYDT(IX)*TEMP3*ALFA + 2.*PI*R(IX)*
         1                     SKC*S1*( 1.-RHOI(IX)/RHOS )*DX
                     DELTA = FLUX(IX) - TEMP0
                     KX = KX + 1
          IF( ABS(DELTA) .LT. SIGMA ) KX = 3
          IF( KX .LT. 3 ) GO TO 110
                     KX = 0
                     UI= ABS(FLUX(IX) )/(PI*R(IX)**2.*RHOI(IX) )
                     UMAX = MAX( UMAX, UI )
                     Y2 = Y3
                     Y3 = 0.
                     DRHO(IX) = TEMP3*ALFA*DYDT(IX)
                     Y(IX) = Y(IX) + DYDT(IX)*DT
                     R(IX) = R(IX) + REGRES(IX)*DT
                     S1 = YSTAR - Y(IX)
          IF ( S1 .GT. 0. ) GO TO 180
                     Y(IX) = YSTAR
                     S1 = 0.
      180 CONTINUE
          IF( IX .EQ. NX ) REMOV=REMOV+ FLUX(IX)*Y(IX)*DT
                     RLOSS = RLOSS + SOLN(IX)*DX
                     ACCUM = ACCUM + PI*RHOI(IX)*Y(IX)*DX*R(IX)**2.
                     DISS = DISS + PI*DX*RHOS*R(IX)**2.
      300 CONTINUE
```

```
                     QWQR = FLUX(NX)
                     FLUX(NNX) = QWQR
                     QW= QWQR/RHOI(NX)
             IF( OUTPUT ) GO TO 400
                GO TO 450
       400           NPR = NPR + 1
             IF( NCOUNT .GT. 1 ) GO TO 405
             READ(5,1017) ( Z(I), I=1,NEXP )
       405 CONTINUE
                     SUB1 = TIME/3600.
                     SUB2 = YFEED/YSTAR
                     SUB3  = QFEED*RHOF/1000.
                     TEMP5 =( 9.+ NX/NDX)*NPR
                     TEMP7 = QFEED/( 16.666*3.78 )
             IF( TEMP5 .LT. 47. ) GO TO 410
             WRITE(6, 1050)
                     NPR= 1
       410 WRITE(6,1055) ( SUB1, IT, TEMP7 )
             WRITE(6,1060)
             WRITE(6,1065)
             WRITE(6,1070) ( SUB2, SUB3 )
                DO 440 IX = 1, NX
                     UI = FLUX(IX)/(RHOI(IX)*PI*R(IX)**2. )
                     SUB4 = R(IX)/100.
                     SUB5 = REGRES(IX)*3600.
                     SUB6 = Y(IX)*100./YSTAR
                     SUB7 = FLUX(IX)/1000.
                     SUB8 = 3600.*DYDT(IX)
                     X1 = IX
                     JEXP = X1
             WRITE(6,1075) ( X1, SUB4, SUB5, SUB6,
           1                Z(JEXP), SUB7, UI, SUB8,
           2                DSALT(IX), RHOI(IX), SOLN(IX), DRAD(IX),
           3                DRHO(IX), BLFLOW(IX), H(IX) )
       440 CONTINUE
                     SUB9 = FLUX(NNX)/1000.
                     SUB10 = REMOV/1000.
                     SUB11 = ACCUM/1000.
                     SUB12 = DISS/1000.
             WRITE(6, 1080) ( SUB9 )
             WRITE(6,1085)
             WRITE(6,1090) ( SUB10, SUB11, SUB12 )
                     OUTPUT = .FALSE.
       450 CONTINUE
                     ADT1 = 1.3*DT1
                     ADT2 = TINC*DX/UMAX
                     DT = AMIN1( ADT1,ADT2 )
       500 CONTINUE
             IF( TIME .LT. TIMPR(ITPR) ) GO TO 90
       600 ENDCAS = .TRUE.
             IF( ENDCAS ) GO TO 700
                GO TO 90
       700 STOP
             END

ND OF COMPILATION:            2 DIAGNOSTICS.
```

```
STORAGE ASSIGNMENT  (BLOCK, TYPE, RELATIVE LOCATION, NAME)

0001   000530 100L     0000   001747 1000F    0000   001757 1005F    0000   002003 1009F    0000   002004 1010F
0000   002013 1013F    0000   002014 1015F    0000   002022 1017F    0001   000554 102L     0000   002024 1020F
0000   002044 1022F    0000   002027 1023F    0000   002035 1024F    0000   002045 1025F    0000   002054 1030F
0000   002060 1035F    0000   002067 1040F    0000   002102 1045F    0001   000700 105L     0000   002104 1050F
0000   002106 1055F    0000   002127 1060F    0000   002170 1065F    0000   002224 1070F    0000   002236 1075F
0001   000631 108L     0000   002251 1080F    0000   002260 1085F    0001   000712 109L     0000   002306 1090F
0001   000730 110L     0001   000761 115L     0001   001011 120L     0001   001015 150L     0001   001020 155L
0001   001043 160L     0001   001047 170L     0001   001153 180L     0001   000106 201G     0001   000114 206G
0001   000127 215G     0001   000147 226G     0001   000264 263G     0001   000304 277G     0001   000336 314G
0001   000363 330G     0001   000375 336G     0001   000435 366G     0001   000503 375G     0001   001222 400L
0001   001241 405L     0001   001303 410L     0001   000611 431G     0001   001475 450L     0001   001235 566G
0001   001521 600L     0001   001341 623G     0001   001525 700L     0001   000442 90L      0000 R 000310 A
0000 R 001703 ACCUM    0000 R 001745 ADT1     0000 R 001746 ADT2     0000 R 001651 ALFA     0000 R 001633 AX
0000 R 001301 BLFLOW   0000 R 001632 CKCP     0000 R 001722 DELTA    0000 R 001702 DISS     0000 R 000625 DRAD
0000 R 001363 DRHO     0000 R 000062 DSALT    0000 R 001660 DT       0000 R 001676 DT1      0000 R 001644 DX
0000 R 000144 DYDT     0000 R 001716 DYT      0000 L 001623 ENDCAS   0000 R 001677 FEED     0000 R 000000 FLUX
0000 R 001217 H        0000 R 001626 HT       0000 I 001641 I        0000 I 001675 IT       0000 I 001636 ITPR
0000 I 001656 IX       0000 I 001674 J        0000 I 001665 JEXP     0000 I 001657 JX       0000 I 001667 KKK
0000 I 001637 KTF      0000 I 001672 KX       0000 I 001710 K1       0000 I 001670 MMM      0000 I 001663 NCOUNT
0000 I 001635 NDX      0000 I 001640 NEXP     0000 I 001671 NNN      0000 I 001655 NNX      0000 I 001664 NPR
0000 I 001627 NT       0000 I 001625 NX       0000 L 001624 OUTPUT   0000 R 001645 PI       0000 R 000771 QCHANG
0000 R 001643 QFEE     0000 R 001630 QFEED    0000 R 001725 QW       0000 R 001724 QWQR     0000 R 000315 R
0000 R 000461 REGRES   0000 R 001662 REMOV    0000 R 001652 RHOF     0000 R 000377 RHOI     0000 R 001650 RHOS
0000 R 001647 RHOW     0000 R 001701 RLOSS    0000 R 001053 RS       0000 R 001666 SIGMA    0000 R 001712 SKC
0000 R 000543 SOLN     0000 R 001541 SUBT     0000 R 001726 SUB1     0000 R 001742 SUB10    0000 R 001743 SUB11
0000 R 001744 SUB12    0000 R 001727 SUB2     0000 R 001730 SUB3     0000 R 001733 SUB4     0000 R 001734 SUB5
0000 R 001735 SUB6     0000 R 001736 SUB7     0000 R 001737 SUB8     0000 R 001741 SUB9     0000 R 001706 S1
0000 R 001707 S2       0000 R 001711 S3       0000 R 001713 S4       0000 R 001631 TEMP     0000 R 001714 TEMP0
0000 R 001715 TEMP1    0000 R 001717 TEMP2    0000 R 001720 TEMP3    0000 R 001721 TEMP4    0000 R 001731 TEMP5
0000 R 001673 TEMP6    0000 R 001732 TEMP7    0000 R 001642 TF       0000 R 001445 TFLOW    0000 R 001661 TIME
0000 R 000707 TIMPR    0000 R 001634 TINC     0000 R 001723 UI       0000 R 001704 UMAX     0000 R 001740 X1
0000 R 000226 Y        0000 R 001646 YFEED    0000 R 001135 YS       0000 R 001654 YSTAR    0000 R 001653 YY
0000 R 001700 Y2       0000 R 001705 Y3       0000 R 001527 Z
```